



Vidya Jyothi Institute of Technology (Autonomous)

(Accredited by NAAC & NBA, Approved By A.I.C.T.E., New Delhi, Permanently Affiliated to JNTU, Hyderabad)
(Aziz Nagar, C.B.Post, Hyderabad -500075)

IV B. Tech II Semester Academic Calendar for the Academic year 2020-21

Department of Mechanical Engineering

Circular

MED/Major Projects/01

Dt: 05/04/2021

All the final year mechanical engineering students are informed that a project work has to be undertaken as partial fulfillment for the award of degree, in this connection you are required to form into groups with three to four members. Grouping is done voluntarily by yourself considering the domain of interest in mechanical engineering. Hence you are required to submit the group along with the domain/project topic so that faculty member can be allocated as supervisor/guide. Also you can speak to the faculty members in choosing them as supervisors for the project work undertaken. The submission of the group to Mr. Prasad Kumar, Asst.Professor, who is project coordinator on or before 20.04.2021

HOD

(Dr.G.Sreeram Reddy)

33	Md Abdul Azeez Azhar	17911A03E2	Experimental investigation on multi fuel single cylinder diesel engine fuelled by diesel-ethanol blends with varying injection timing and multiple injection	P Chandra kumar	CBIT	PO1,PO2,PO3,PO4,PO5,PO9,PO12
	Mohammed Azhar	17911A03E3				
	Muddasir Ahmed	17911A03E4				
	Md Ameer Ali	17911A03E5				
34	A v S Krishna Yeshwanth	17911A03B2	Stress analysis of notched super duplex stainless UNS S32760	Dr.J.Jagadesh Kumar	CBIT	PO1,PO2,PO3,PO4,PO5,PO9,PO12
	Ch Premraj	17911A03C7				
	V Akilesh	17911A03F6				
	TS Adheesh	17911A0351				
35	B Sai tarun reddy	17911A03B9	Eperimental investigation of CNG enriched automotive CRDI dual fuel diesel engine with waste plastic oil biodiesel blends	K Ravi kumar	CBIT	PO1,PO2,PO3,PO4,PO5,PO9,PO12
	R Teja guptha	17911A03E8				
	M Chandu prakash Reddy	17911A03D7				
	V Sai kiran chary	17911A03F7				
36	Bhukya Ramesh	17911A03C2	Design of an automatic fire extinguisher robot	Shaik Saidulu	VJIT	PO1,PO2,PO3,PO4,PO9,PO12,PSO 1
	M Bharath kumar Reddy	17911A03E2				
	B Praveen kumar	18915A0305				
	P Pavan kumar	17911A03E7				
37	D Sanjith Reddy	17911A03D0	Design and modelling of Rocker-Nogie mechanism	Dr.Sudhabindu	CBIT	PO1,PO2,PO3,PO4,PO9,PO12
	M Sai Chandranath	17911A03C0				
	P Sainath	17911A03F0				
	K Vamshi Krishna Reddy	17911A03D5				
38	Md Mohammed Ali	17911A0329	Design, modeling and analysis of automatic car parking system	Dr.V V Sathyanarayana	VJIT	PO1,PO2,PO3,PO4,PO9,PO12
	Shaik Abdul Waseem	18915A0346				
	Mohammed moizuddin	17911A0335				
	Tauseef mohammed tayyab	17911A0352				
39	M Nikhil goud	17911A03D8	Design and fabrication of regenerative braking system	S Venkatesh	VJIT	PO1,PO2,PO3,PO4,PO9,PO12,PSO 1
	B Manish Reddy	17911A03B6				
	C Manish goud	17911A03C5				
	G Dheeraj kumar	17911A03D1				
40	B Hrithik Varma	17911A033B8	Thermal analysis of an exhaust valve of an IC engine using different materials	Shail Ismail	VJIT	PO1,PO2,PO3,PO4,PO9,PO12
	Guguloth kumar	17911A03D3				
	T Madhusudan Reddy	17911A03F5				
	D Vikram	18915A0310				

RUBRICS FOR EVALUATION OF PROJECTS

Criterion for Evaluation/ Rubric	Poor (1)	Satisfactory (2)	Good (3)	Very Good (4)	Excellent (5)
Requirements	Project does not adhere to its requirements.	Project minimally adheres to its requirements.	Project mostly adheres to its requirements	Project completely adheres to its requirements	Project completely adheres to its requirements and suits current day's industry needs.
Creativity	Project is significantly incomplete and lacking creativity.	Project is somewhat incomplete and slightly creative.	Project is complete and creative.	Project is complete, creative and novel.	Project is highly creative and visibly appealing.
Model Building	Contains no involvement of mechanical engineering concepts.	Contains minimal involvement of mechanical engineering concepts.	Contains involvement of mechanical engineering concepts in study-oriented approach.	Contains involvement of mechanical engineering concepts like design, fabrication, analysis etc. without any live model or simulation.	Contains involvement of mechanical engineering concepts like design, fabrication, analysis etc and working model/ simulation as well.
Quality of the work	Project is of poor quality work.	Project appears hastily created or is of poor quality work.	Project construction could benefit from more than a minimal amount of effort.	Project construction could be improved somewhat in select areas.	Project is of excellent, durable construction.

92	17911A03B2	Stress analysis of Notched super duplex stainless steel UNS S32760.	10	10	14	34
93	17911A03B3	Enhancing the mechanical properties of polymer based Hybrid Composite Material.	11	12	14	37
94	17911A03B4	Design and fabrication of Solar wood cutter	12	13	14	39
95	17911A03B5	Thermal analysis of an exhaust valve of an IC engine using different materials.	12	14	15	41
96	17911A03B6	Design and fabrication of Regenerative braking system.	10	13	16	39
97	17911A03B7	Study and Fabrication of waterlily Turbine.	11	12	16	39
98	17911A03B8	Thermal analysis of an exhaust valve of an IC engine using different materials.	11	11	16	38
99	17911A03B9	Experimental investigation of CNG enriched automotive CRDi dual fuel diesel engine with plastic oil biodiesel blends.	10	13	15	38
100	17911A03C1	Design and fabrication of Solar wood cutter	10	11	15	36
101	17911A03C2	Design of an automatic fire extinguisher robot.	12	12	14	38
102	17911A03C3	Modelling and analysis of a Centrifugal Impeller.	11	10	16	37
103	17911A03C4	Thermal analysis of an exhaust valve of an IC engine using different materials.	12	13	14	39
104	17911A03C5	Design and fabrication of Regenerative braking system.	11	13	15	39
105	17911A03C6	Thermal analysis of an exhaust valve of an IC engine using different materials.	12	14	15	41
106	17911A03C7	Stress analysis of Notched super duplex stainless steel UNS S32760.	12	13	15	40
107	17911A03C8	Design and fabrication of Solar wood cutter	11	13	15	39
108	17911A03C9	Study and Fabrication of waterlily Turbine.	10	11	16	37
109	17911A03D0	Design and modelling of Rocker-Bogie mechanism.	11	11	15	37
110	17911A03D1	Design and fabrication of Regenerative braking system.	10	12	14	36
111	17911A03D2	Modelling and analysis of a Centrifugal Impeller.	11	13	14	38
112	17911A03D3	Thermal analysis of an exhaust valve of an IC engine using different materials.	12	13	15	40
113	17911A03D4	Modelling and analysis of a Centrifugal Impeller.	11	14	16	41
114	17911A03D5	Design and modelling of Rocker-Bogie mechanism.	12	13	16	41
115	17911A03D6	Modelling and analysis of a Centrifugal Impeller.	10	13	17	40
116	17911A03D7	Experimental investigation of CNG enriched automotive CRDi dual fuel diesel engine with plastic oil biodiesel blends.	11	13	15	39
117	17911A03D8	Design and fabrication of Regenerative braking system.	12	11	18	41
118	17911A03D9	Study and Fabrication of waterlily Turbine.	10	12	14	36
119	17911A03E0	Design and modelling of Rocker-Bogie mechanism.	11	13	15	39
120	17911A03E1	Design of an automatic fire extinguisher robot.	12	11	16	39
121	17911A03E2	Experimental investigation on multi fuel single cylinder diesel engine fuelled by diesel-ethanol blends with varying injection timing and multiple injection.	11	13	16	40
122	17911A03E3	Experimental investigation on multi fuel single cylinder diesel engine fuelled by diesel-ethanol blends with varying injection timing and multiple injection.	10	12	16	38
123	17911A03E4	Experimental investigation on multi fuel single cylinder diesel engine fuelled by diesel-ethanol blends with varying injection timing and multiple injection.	12	11	17	40
124	17911A03E5	Experimental investigation on multi fuel single cylinder diesel engine fuelled by diesel-ethanol blends with varying injection timing and multiple injection.	11	13	16	39
125	17911A03E7	Design of an automatic fire extinguisher robot.	12	13	16	41
126	17911A03E8	Experimental investigation of CNG enriched automotive CRDi dual fuel diesel engine with plastic oil biodiesel blends.	11	13	17	41
127	17911A03E9	Enhancing the mechanical properties of polymer based Hybrid Composite Material.	10	11	17	38
128	17911A03F0	Design and modelling of Rocker-Bogie mechanism.	12	12	16	40
129	17911A03F1	Design and fabrication of Solar wood cutter	10	13	16	39
130	17911A03F2	Enhancing the mechanical properties of polymer based Hybrid Composite Material.	11	12	14	37
131	17911A03F4	Investigation of mechanical properties of friction stir welding of Aluminium alloy 6063 using cerium powder.	10	11	15	36
132	17911A03F5	Thermal analysis of an exhaust valve of an IC engine using different materials.	12	11	15	38
133	17911A03F6	Stress analysis of Notched super duplex stainless steel UNS S32760.	10	12	14	36
134	17911A03F7	Design of an automatic fire extinguisher robot.	11	11	15	37
135	17911A03F8	Enhancing the mechanical properties of polymer based Hybrid Composite Material.	12	11	15	38
136	17911A03F9	Design and implementation of Low-cost 2d plotter computer numeric Control machine.	12	13	15	40
137	17911A03G0	Design analysis and fabrication of Multipoint cutting tool.	10	12	16	38
138	17911A03G1	Design and fabrication of portable Air conditioner.	12	12	16	40
139	17911A03G2	Design and fabrication of Solar Air Heater.	11	11	17	39
140	17911A03G3	Fabrication of Automatic sanitizing equipment.	11	12	16	39
141	17911A03G5	Comparative Evaluation of Mild steel welded joints Employed by different processes.	10	10	16	36
142	17911A03G6	Design and fabrication Solar grass cutter.	11	13	16	40
143	17911A03G7	Design and Fabrication of Electronic Braking System.	11	13	14	38
144	17911A03G8	Design and Fabrication of Electro Magnetic Suspension System.	12	13	16	41
145	17911A03H0	Design and fabrication Solar grass cutter.	11	12	17	40
146	17911A03H1	Synthesis and characterization of magnetic Nano particles using Novel Arc discharge method.	12	12	16	40
147	17911A03H2	Design and Fabrication of Electro Magnetic Suspension System.	11	13	16	40
148	17911A03H3	Fabrication of Automatic sanitizing equipment.	11	12	15	38
149	17911A03H4	Design and fabrication of Solar Air Heater.	12	13	15	40
150	17911A03H5	Enhancing the mechanical properties of polymer based Hybrid Composite Material.	10	12	18	40



VIDYA JYOTHI INSTITUTE OF TECHNOLOGY (AUTONOMOUS)

(Accredited by NAAC & NBA, Approved By A.I.C.T.E., New Delhi, Permanently Affiliated to JNTU, Hyderabad)
(Aziz Nagar, C.B Post, Hyderabad -500075)

Department of Mechanical Engineering

IV YEAR PROJECT REVIEW MARKS

YEAR: 2020-21

S.No	H.T.NO	PROJECT TITLE	Review I (15)	Review II (15)	Review III (20)	Total (50)
1	17911A0301	Crush tubes for near-ideal vehicular crash energy absorption.	13	13	16	42
2	17911A0302	Design and Fabrication of snake robot.	12	12	15	39
3	17911A0306	Design and Fabrication of snake robot.	13	12	16	41
4	17911A0308	Design, Analysis & fabrication of High speed Motorized spindle.	12	11	14	37
5	17911A0309	Design and Fabrication of snake robot.	13	12	15	40
6	17911A0312	Design and analysis of automatic garbage collector machine.	12	12	14	38
7	17911A0313	Fabrication and testing of Multi directional unloading dump truck with auto sensing and alert system.	11	13	14	38
8	17911A0314	Design and analysis of automatic garbage collector machine.	12	13	12	37
9	17911A0315	Impact of split injection strategy on combustion performance characteristics of biodiesel fueled Automotive CRDI research engine,	12	11	16	39
10	17911A0317	Design, Analysis & fabrication of High speed Motorized spindle.	12	12	14	38
11	17911A0319	Impact of split injection strategy on combustion performance characteristics of biodiesel fueled Automotive CRDI research engine,	11	13	14	38
12	17911A0320	Fabrication and testing of shell and tube heat exchanger.	12	13	14	39
13	17911A0321	Design and Fabrication of snake robot.	13	11	15	39
14	17911A0322	Experimentation on fracture toughness of raw jute and hybrid jute composite using SNEB specimens.	12	13	15	40
15	17911A0323	Design, Analysis & fabrication of High speed Motorized spindle.	12	11	13	36
16	17911A0324	Design and analysis of automatic garbage collector machine.	11	12	16	39
17	17911A0325	Design and Fabrication of snake robot.	12	11	14	37
18	17911A0327	Fabrication and testing of Multi directional unloading dump truck with auto sensing and alert system.	11	12	13	36
19	17911A0328	Fabrication and testing of Multi directional unloading dump truck with auto sensing and alert system.	12	11	15	38
20	17911A0329	Design Modelling and analysis of automatic car parking.	11	10	13	34
21	17911A0330	Fabrication and testing of Multi directional unloading dump truck with auto sensing and alert system.	12	10	16	38
22	17911A0331	Modelling and analysis of a wheel Rim.	12	11	14	37
23	17911A0332	Modelling and analysis of a wheel Rim.	12	13	16	41
24	17911A0333	Modelling and analysis of a wheel Rim.	11	12	16	39
25	17911A0334	Modelling and Analysis of J beams.	12	11	15	38
26	17911A0335	Design Modelling and analysis of automatic car parking.	10	12	14	36
27	17911A0336	Modelling and analysis of a wheel Rim.	11	12	14	37
28	17911A0337	Modelling and Analysis of J beams.	10	12	14	36
29	17911A0338	Crush tubes for near-ideal vehicular crash energy absorption.	11	12	14	37
30	17911A0339	Synthesis and characterization of magnetic Nano particles using Novel Arc discharge method.	11	12	17	40
31	17911A0340	Impact of split injection strategy on combustion performance characteristics of biodiesel fueled Automotive CRDI research engine,	11	12	15	38
32	17911A0341	Experimental investigation on Mechanical properties of Austenitic Stainless steel joints of SS304 & SS316 using Plasma Arc welding.	12	14	16	42
33	17911A0342	Experimentation on fracture toughness of raw jute and hybrid jute composite using SNEB specimens.	12	13	16	41
34	17911A0343	Design, Analysis & fabrication of High speed Motorized spindle.	11	12	14	37
35	17911A0344	Experimentation on fracture toughness of raw jute and hybrid jute composite using SNEB specimens.	12	13	14	39
36	17911A0345	Fabrication and testing of shell and tube heat exchanger.	12	13	15	40
37	17911A0346	Design Modelling and analysis of automatic car parking.	12	11	16	39
38	17911A0347	Fabrication and testing of shell and tube heat exchanger.	11	13	15	39
39	17911A0349	Design and analysis of automatic garbage collector machine.	10	12	13	35
40	17911A0350	Modelling and Analysis of J beams.	11	12	15	38
41	17911A0351	Stress analysis of Notched super duplex stainless steel UNS S32760.	12	12	15	39
42	17911A0352	Design Modelling and analysis of automatic car parking.	11	13	14	38
43	17911A0354	Modelling and Analysis of J beams.	12	12	15	39
44	17911A0355	Crush tubes for near-ideal vehicular crash energy absorption.	10	12	15	37
45	17911A0356	Crush tubes for near-ideal vehicular crash energy absorption.	12	13	16	41
46	17911A0358	Fatigue analysis of notched super Austenitic stainless steel UN S31254.	11	13	15	39
47	17911A0359	Design and analysis of Universal gearless power transmission mechanism.	11	12	15	38
48	17911A0360	Experimental investigations on wear behaviour of kenaf-epoxy & kenaf-basalt epoxy hybrid lamination.	12	13	15	40

VIDYA JYOTHI INSTITUTE OF TECHNOLOGY

DEPARTMENT OF MECHANICAL ENGINEERING

Date: 10.07.2021

CIRCULAR

As an initiative by the department of mechanical engineering in the identification of best projects, a selection committee has been constituted to review and scrutinize all the projects for the academic year 2020-2021, based on following factors.

1. Creativity
2. Type of Materials used
3. Manufacturing Methods Employed
4. Experimentation results through design of experiments
5. Analysis of results
6. Conclusion

The prospective projects selected are taken for award to be conferred.

The committee members are:

1. Dr. V.V. Satyanarayana



2. Dr. L. Madan Anand kumar



3. Dr. V Phanindra Bogu



HoD/MECH



VIDYA JYOTHI INSTITUTE OF TECHNOLOGY

DEPARTMENT OF MECHANICAL ENGINEERING

Date: 22.07.2021

CIRCULAR

After thorough reviewing of all the projects by considering following factors, the committee members has selected the best projects for which award is to be conferred on 15.07.2021.

1. Creativity
2. Type of Materials used
3. Manufacturing Methods Employed
4. Experimentation results through design of experiments
5. Analysis of results
6. Conclusion

The Best Projects are:

S.NO	H.T.No.	NAME OF THE STUDENT	PROJECT TITLE	GUIDE
1	17911A03H9	K Vamshi Reddy	Fabrication of Automatic sanitizing equipment	Dr. B.V. Reddy
	17911A03J4	M Prajeet		
	17911A03K3	P S Anand Krishnan		
	17911A03H3	C. Ravindar Reddy		
2	17911A03J9	Naganand Shenoy	Deviation analysis of A free form surface using reverse engineering approach	Dr. G. Sreeram Reddy
	17911A03K0	N Aranvid Kumar		
	17911A0399	P Sharavan Kumar		
	17911A03LO	S. Uday Kumar		
	17911A03J1	K Durga Prasad		
3	17911A03B2	AV S Krishna Yeshwanth	Stress anaysis of notched super duplex stailless steel UNS S32760	Dr. J. Jagadesh Kumar
	17911A03C7	Ch. Premraj		
	17911A03F6	V Akhilesh		
	17911A0351	T S Adheesh		

HoD/MECH
f

VIDYA JYOTHI INSTITUTE OF TECHNOLOGY

DEPARTMENT OF MECHANICAL ENGINEERING

MAIN PROJECT BATCHES WITH GUIDES 2020-2021

SECTION-C

Batch	H.T.No.	Name of the Student(s)	Marks / Grade	Name of the Guide	Title of the project
1	17911A03E2	Md Abdul Azeez Azhar	B	P.Chandra Kumar	Experimental investigation on multi fuel single cylinder diesel engine fuelled by diesel- ethanol blends with varying injection timing and multiple injection
	17911A03E3	Mohammed Azher	B		
	17911A03E4	Muddasir Ahmed	B		
	17911A03E5	Md Amer Ali	B		
2	17911A03B2	A V S Krishna Yeshwanth	O	Dr.J Jagadesh Kumar	STRESS ANALYSIS OF NOTCHED SUPER DUPLEX STAINLESS STEEL UNS S32760
	17911A03C7	Ch. Premraj	O		
	17911A03F6	V Akhilesh	O		
	17911A0351	T S Adheesh	O		
3	17911A03B9	B.Sai Tharun Reddy	A	Mr.K.Ravi Kumar	Experimental investigation of CNG enriched automotive CRDi dual fuel diesel engine with waste plastic oil biodiesel blends
	17911A03E8	R.Teja Gupta	A		
	17911A03D7	M Chandu Prakash Reddy	A		
	17911A03F7	V.Sai Kiran Chary	A		
4	17911A03C2	bhukya ramesh	B	Mr Shaik Saidulu	DESIGN OF AN AUTOMATIC FIRE EXTINGUISHER ROBOT
	17911A03E1	m.bharath Kumar Reddy	B		
	18915A03D5	Bhyn Praveen Kumar	B		
	17911A03E7	poturi.pavankumar	B		
5	17911A03D0	D.Sanjith Reddy	B	Dr. B. Sudha Bindu	Design and modelling of ROCKER-BOGIE mechanism
	17911A03E0	M.Sai Chandranath	B		
	17911A03F0	P.Sainath	B		
	17911A03D5	K.Vamshi Krishna Reddy	B		

[Signature]

[Signature]

[Signature]

A Project Report on

STRESS ANALYSIS OF NOTCHED SUPER DUPLEX STAINLESS STEEL UNS S32760

Submitted in partial fulfillment of the requirement for the award of the degree of

BACHELOR OF TECHNOLOGY

in

MECHANICAL ENGINEERING

by

A.V.S. KRISHNA YESHWANTH	17911A03B2
T.S. ADHEESH	17911A0351
V. AKHILESH	17911A03F6
CH. PREMRAJ	17911A03C7



Under the esteemed guidance of

Dr. J. Jagadesh Kumar

Associate Professor

Submitted to

DEPARTMENT OF MECHANICAL ENGINEERING
VIDYA JYOTHI INSTITUTE OF TECHNOLOGY

(An Autonomous Institution)

Approved by AICTE New Delhi & Permanently Affiliated to JNTUH, Accredited by NAAC & NBA, An
ISO 9001:2015 Certified Institution

Aziz Nagar Gate, C.B. Post, Hyderabad-500 075

(2020-21)

DEPARTMENT OF MECHANICAL ENGINEERING

VIDYA JYOTHI INSTITUTE OF TECHNOLOGY

(An Autonomous Institution)

Approved by AICTE New Delhi & Permanently Affiliated to JNTUH, Accredited by NAAC & NBA, An ISO 9001:2015 Certified Institution

Aziz Nagar Gate, C.B. Post, Hyderabad-500 075



BONAFIDE CERTIFICATE

This is to certify that the project work entitled “**STRESS ANALYSIS OF NOTCHED SUPER DUPLEX STAINLESS STEEL UNS S32760**” is submitted by **A V S KRISHNA YESHWANTH (17911A03B2), T.S ADHEESH (17911A0351), V AKHILESH (17911A03F6), CH PREMRAJ (17911A03C7)** in the department of Mechanical Engineering in partial fulfillment of requirements for the award of degree of Bachelor of Technology in Mechanical Engineering for the academic year 2020-21. This work has been carried out under my guidance and has not been submitted the same for any university/institution for award of any Degree/Diploma.

INTERNAL GUIDE

Dr. J. JAGADESH KUMAR

(Associate Professor)

HEAD OF DEPARTMENT

Dr. G. SREERAM REDDY

(Head of Dept. of Mechanical Engineering.)

Head of Department
Mechanical Engineering
VIDYA JYOTHI INSTITUTE OF TECHNOLOGY
HYDERABAD-500 075

EXTERNAL EXAMINER

ACKNOWLEDGEMENT

We take this opportunity to thank Dr. E. Sai Baba Reddy, Director - VJIT, Dr. G. Sreeram Reddy, HOD Mechanical Department, and our guide Dr. J. Jagadesh Kumar who guided us throughout our project.

We extend our sincere thanks to one and all of VJIT family for the completion of this document on the project report as per guidelines

A V S KRISHNA YESHWANTH 17911A03B2

T. S ADHEESH 17911A0351

C.H PREMRAJ 17911A03C7

V AKHILESH 17911A03F6

DECLARATION

This is to certify that the work reported in the presented project entitled “**STRESS ANALYSIS OF NOTCHED SUPER DUPLEX STAINLESS STEEL UNS S32760**” is a record of the work done by us in the Department of Mechanical Engineering, Vidya Jyothi Institute of Technology, affiliated to Jawaharlal Nehru Technological University, Hyderabad. The report is based on the project work done entirely by us and not copied from any other source.

PROJECT ASSOCIATES:

A V S KRISHNA YESHWANTH 17911A03B2

T. S ADHEESH 17911A0351

V. AKHILESH 17911103F6

C.H. PREMRAJ 17911A03C7

TABLE OF CONTENTS

DESCRIPTION	PAGE NUMBER
CERTIFICATE	i
ACKNOWLEDGEMENTS	ii
ABSTRACT	iv
LIST OF FIGURES	viii
LIST OF TABLES	x
1. INTRODUCTION	1-3
1.1 Fatigue failure mechanism	1
1.2 Models of fatigue life estimation	1
1.3 Current project problem	3
1.4 Outline of the thesis	3
1.5 Objectives of the project	3
2. LITERATURE SURVEY	4-19
2.1 Fatigue	4
2.2 Historic overview of fatigue	8
2.3 Effect of notch on fatigue life of steels	12
2.4 Fatigue life predication methods	13

2.5 Fatigue analysis using finite element method	16
2.6 Stainless steels	18
3. MATERIALS AND METHODS	20-25
3.1 Material used	20
3.2 Grades of duplex steels	20
3.3 UNS s32760	21
3.4 Methods	23
4. NUMERICAL METHODS	26-37
4.1 Prediction of axial fatigue life from tensile data	26
4.2 Four-point correlation method	26
4.3 Muralidharan-Manson method	30
4.4 Roessle and Fatemi hardness method	31
4.5 Mitchell's method	32
4.6 Meggiolaro and Castro method	33
4.7 Strain life plots	33
5. FINITE ELEMENT METHOD	38-48
5.1 Meshing	38
5.2 Loading	38

5.3 Strain based analysis in ANSYS	39
5.4 Boundary conditions	41
5.5 Material assignment	42
5.6 Notch variations	42
5.7 Solution	43
6. RESULTS	49-54
6.1 Taguchi optimization	49
6.2 Regression analysis	50
6.3 Response surface methodology	51
7. CONCLUSION	55
8. REFERENCES	56

LIST OF FIGURES

FIGURE NUMBER	TITLE	PAGE NUMBER
1.1	Stress life data and curve fit vs strain life data and curve fit	2
2.1	Cyclic loading	6
2.2	Phases in fatigue failure	14
3.1	Light optical micro graph of super duplex steels	22
4.1	Strain range vs cycles to failure	26
4.2	Strain range vs cycles to failure indicating four-point correlation method	26
4.3	True fracture stress vs the approximation of John O' Brien	28
4.4	Ratio of UTS and E vs % reduction in area	28
4.5	Strain life plot using modified four-point correlation method	34
4.6	Strain life plot using modified universal slopes method	34
4.7	Strain life plot using hardness method	35
4.8	Strain life plot using Mitchell's method	35
4.9	Strain life plot using median method	36
4.10	Comparison of numerical methods	36
5.1	Standard fatigue test specimen with meshing	38
5.2	Loading on the standard specimen	39
5.3	Constant amplitude fully reversed loading	39

5.4	Specification of strain life analysis in the fatigue tool	40
5.5	Mean stress correction	41
5.6	Boundary conditions on fatigue specimen	41
5.7	Different variations of V-notch and resulting fatigue life and equivalent stress	43
5.8-5.17	Equivalent stress and fatigue life contours of test specimen	44-48
6.1	Variation of fatigue life with width, depth and notch central angle	49
6.2	Surface plot of fatigue life vs width vs depth	52
6.3	Surface plot of fatigue life vs notch central angle vs depth	52
6.4	Surface plot of fatigue life vs width vs notch central angle	53
6.5	Contour plot of fatigue life vs depth and width	53
6.6	Contour plot of fatigue life vs depth and notch central angle	54
6.7	Contour plot of fatigue life vs notch central angle and width	54

LIST OF TABLES

TABLE NUMBER	TITLE	PAGE NUMBER
2.1	Classification of stainless steels	18
3.1	Factors chosen and their levels	24
3.2	Notch parameters for fatigue analysis	25
4.1	Materials for axial low fatigue investigation	29
4.2	Material variables in axial low cycle fatigue investigation	29
6.1	Response table	49
6.2	ANOVA of Taguchi method	50
6.3	ANOVA of RSM	51

CHAPTER 1: INTRODUCTION

Fatigue is defined as a failure under a repeated load which never reaches a level sufficient to cause failure in a single application. The word fatigue originates from Latin expression “fatigue” which means “to tire”. The terminology used in engineering refers to the damage and failure of materials under cyclic loads including mechanical loads, thermal loads and so forth. Fatigue damage characterized by nucleation, coalescence, and stable growth of cracks, leading ultimately to net section yielding or brittle fracture.

1.1 MECHANISM

Fatigue failure is the deterioration of a material as a result of cyclic loading which causes progressive and localized structural damage followed by the growth of cracks. A crack that had instigated will grow in a diminutive fashion in each and every load cycle until it attains a critical size that happens when the cracks stress intensity factor surpasses the fracture toughness of the material. This results in speedy propagation and usually complete fracture of the component/structure. Fatigue has conventionally been linked to failure of metallic structures and this led to the term “metal fatigue”.

1.2 MODELS OF FATIGUE LIFE ESTIMATION

- Stress based approach
- Strain based approach

Stress life methods are most useful at high cycle fatigue, where the applied stresses are elastic, and no plastic strain occurs anywhere other than at the tips of fatigue cracks. At low cycles, scatter in the fatigue data makes these methods increasingly less reliable. On the other hand, strain life methods can be used for low cycle fatigue, where there the loading is a combination of elastic and plastic on the macro scale. For most stress life calculations, the math is relatively easy, since there is only one stress component. In strain life calculations, the math is more difficult, as the elastic and plastic components of the strain must be dealt with separately

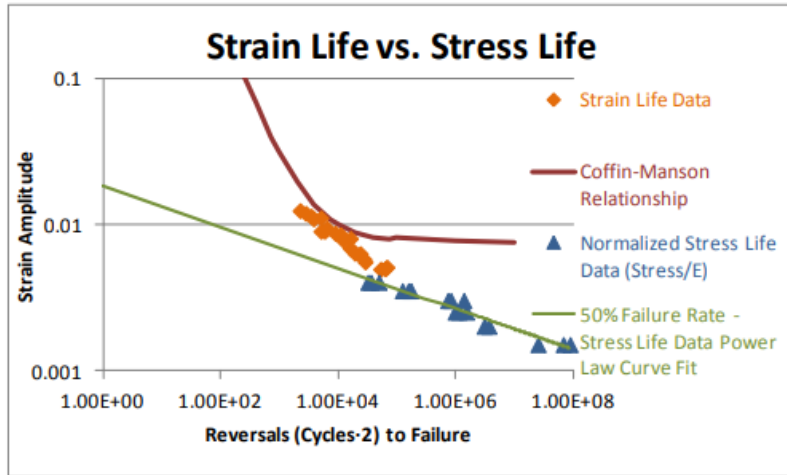


Fig 1.1 Stress Life Data and Curve Fit vs. Strain Life Data and Curve Fit

The diagram shows that there is not an "apples to apples" correlation between the two methods. This is even after the stress life data are converted by dividing stress amplitude by elastic modulus to obtain an equivalent strain amplitude, and the cycles to failure are multiplied by two to obtain reversals to failure. Part of this is due to the fact that the fully reversed stress life data were obtained in bending, and the strain life data was obtained in tension.

Stress life and strain life test data often do not correlate well to each other, as shown above in Figure 1.1. The data points are for the same material, albeit different forms. The strain life data were measured in relatively thick plate, while the stress life data were measured in thin strip, which may account for some additional differences. In order to attempt a reasonable comparison, the stress amplitude data points from the stress life method were divided by the elastic modulus of the material to convert them to strain amplitude. Additionally, the stress life cycles to failure were multiplied by two to obtain reversals to failure. Note that the data points do not quite line up, as well as the different shapes of the curve fits used for the different techniques. Again, remember that stress life techniques are not used in low cycle (below about 10^4 cycles). The stress-life curve fit below indicates why, as it does not account for the ability to handle greater strain amplitudes at low cycles.

Though many engineering structures are built based on standard rules and stress-based approaches, failures are still observed due to fatigue. Due to the large uncertainties like varied wave environments, uncertain hydro-dynamic repetitive loads, stress concentrations etc. involved in the fatigue design process of ships and aircraft, fatigue cracks occur much earlier than expected. One of the reasons for the deficient fatigue design of ships and aircraft is the absence/ insufficient usage of strain-based approaches during fatigue studies. The presence of

sudden geometry changes, notches and cracks on the surface 2 also need to be given weightage during the fatigue design. Hence design of these structures for fatigue loading is insufficient without strain-based fatigue analysis.

1.3 CURRENT PROJECT PROBLEM

Current project aims to investigate the fatigue life of notched super duplex stainless steel UNS s32760. The notch parameters width, depth and notch central angle were varied in finite element analysis done in ANSYS 2020 R2. The fatigue life and the equivalent stress generated were investigated for each variation of 27 types of V notched specimen.

1.4 OUTLINE OF THE THESIS

The current thesis is presented in the following manner for lucidity. Chapter 3 includes the material details and the methods used. Chapter 4 has the details of the numerical methods where the information related to the fatigue properties of the material and their formulae. Chapter 5 deals with finite element analysis to estimate the equivalent (von mises) stress and fatigue life. Chapter 6 encompasses the analysis and results of the previously obtained FEM data. Chapter 7 deals with the conclusion of the project and discussion of further scope.

1.5 OBJECTIVES OF THE PROJECT

The objectives of the current project are to carry out:

- Objective-1: Stress analysis of super duplex stainless steel using empirical methods
- Objective-2: Stress analysis of super duplex stainless steel with FEM.
- Objective-3: Quantification of the influence of notch parameters which are width, depth and notch central angle on the fatigue life for the chosen material by using DOE approach.
- Objective-4: Prediction of the impact of any notch variant on the fatigue life using regression analysis.

CHAPTER 2: LITERATURE SURVEY

2.1. FATIGUE

Fatigue is slow, restricted, and permanent failure that happens in a component exposed to fluctuating stresses that are often much lower in magnitude than the material's tensile strength. Fatigue loading may initially create cracks and cause fracture after an adequate number of fluctuations. Fatigue failure consists of three stages:

- Preliminary fatigue failure and initiation of crack.
- Propagation of the crack to a critical size.
- Ultimate abrupt fracture in the residual cross-section.

Damage due to fatigue loading is instigated by the simultaneous acts of cyclic stress, plastic strain and tensile stress. If any of these is absent, fatigue crack does not crop up and propagate. The plastic strain which is a consequence of cyclic stress causes the crack and the tensile stress makes the crack to propagate. Vigilant quantification of strains depicts that plastic strains though microscopic in nature could exist even at lower magnitudes of stress where the strain if observed at macroscopic level appear to be totally elastic.

Even though compressive stresses do not cause fatigue failure, compressive loads may crop up local tensile stresses. Fatigue strength of steels is generally considered to be proportional to hardness and tensile strength, but this generalization may not be factual always. Processing operations, fabrication methods, heat/surface treatments, finishing done, and service conditions profoundly impact the behaviour of a material exposed to cyclic loading. Forecasting the fatigue life of a component is complex as materials are usually sensitive towards minor variations in loading pattern, stress concentrations etc.

Any component's resistance to fatigue damage is dependent even upon the manufacturing methodology (forming, brazing, welding, machining etc.) and surface conditions like roughness and the amount of residual stresses present. Fatigue tests undertaken using small specimens are insufficient to exactly estimate the fatigue life of materials/components. These can be helpful in evaluating the resistance of a material towards cyclic stressing. Apart from material properties and magnitude of loads, the criteria for design must take into cognizance, the type of loading applied, load pattern, overall dimensions of the part, fabrication methodology, magnitude of peak stresses, surface roughness, corrosion impact, temperature of operation, environment, defects induced due to service etc.

Customarily, fatigue life is articulated as the count of stress cycles needed for a crack to initiate and develop big enough to produce the disastrous breakdown i.e., parting into two pieces. B. Boardman et. al., expressed fatigue data as a function of total life that holds good for small laboratory samples but for real components, crack initiation may occur in very few cycles when compared to the total life of the component. Fatigue data can as well be articulated as a function of crack growth rate. Earlier, it was presumed commonly that total fatigue life entailed primarily, the crack initiation phase which is the first stage of fatigue failure, and the time needed for the tiny fatigue crack to develop and cause failure was a small fraction of the total life. However, with the advancements in crack detection methods, it was found that cracks often develop as early as after 10% of total lifetime and grow endlessly till complete failure happens. This finding inspired researchers to use the growth rate of crack for the forecast of total fatigue life. The occurrence of fatigue failures can be significantly reduced by cautious consideration to design particulars and manufacturing procedures. The utmost worthwhile and cost effective method of enhancing fatigue performance is upgrading the design to:

- Eradicate or diminish stress raisers through restructure of the part.
- Avoid shrill surface tears cropping up from various machining processes.
- Avoid surface discontinuities during processing or heat treatment.
- Balance the residual stresses triggered by fabrication and heat treatment processes.
- Improvise fabrication and fastening methods.

Fatigue failure was first identified as a hitch in the first half of 19th century after engineers of Europe had detected the cracks in different bridge and railroad mechanisms which were exposed to repeated loading. As the time advanced and the utilization of metals increased with the growing use of machines, numerous failures in structures/components exposed to repeated loads were chronicled. Today, fatigue analysis gained further prominence as a result of the increase in the usage of novel high-strength materials and the requirement of superior performance of members made of these materials.⁷ The three primary factors that can cause fatigue failure are

- (1) a tensile stress of adequately high value
- (2) a large fluctuation in the applied stress, and

(3) a huge number of applied stress cycles.

There are several types of fluctuating stresses and a fully reversed stress cycle where the maximum and minimum stress magnitudes are equal, as shown in the Fig. 2.1, is frequently used for experimental fatigue testing.

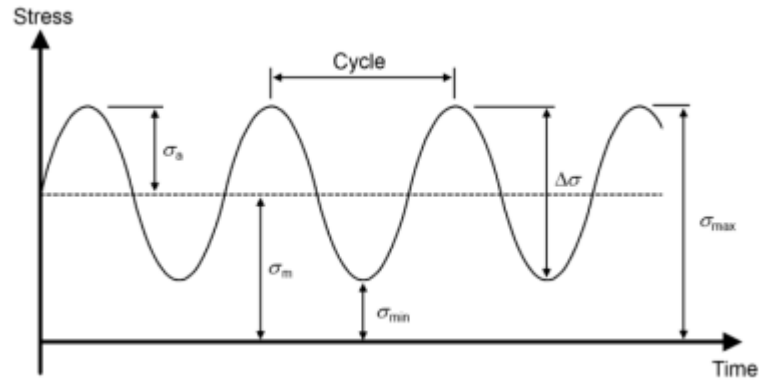


Fig 2.1 Cyclic Loading

2.1.1. Terminology in Fatigue

Stress Range: The stress range, σ_r is given by the maximum stress minus the minimum stress in a cycle;

$$\sigma_r = \sigma_{max} - \sigma_{min} \quad (Equ. 2.1)$$

Alternating Stress: The alternating stress σ_a is given by $0.5\sigma_r$.

$$\sigma_a = \frac{\sigma_r}{2} = \frac{\sigma_{max} - \sigma_{min}}{2} \quad (Equ. 2.2)$$

Mean Stress: The mean stress σ_m is the mean of the maximum and minimum stress in a cycle:

$$\sigma_m = \frac{\sigma_{max} + \sigma_{min}}{2} \quad (Equ. 2.3)$$

Stress Ratio: The stress ratio R is given by the ratio of σ_{max} and σ_{min} ;

$$R = \frac{\sigma_{max}}{\sigma_{min}} \quad (Equ. 2.4)$$

Amplitude Ratio: The amplitude ratio A is the ratio of σ_a and σ_m ;

$$A = \frac{\sigma_a}{\sigma_m} = \frac{1-R}{1+R} \quad (Equ. 2.5)$$

Fatigue Strength: Fatigue strength (endurance limit) is the stress less than which fatigue failure is not observed.

High Cycle Fatigue:

High-cycle fatigue failure happens after a large number of cycles (usually $N > 10^4$ or 10^5 cycles) and stresses induced are mostly elastic in nature. High-cycle fatigue test runs are normally undertaken for 10^7 cycles and in some cases 8 up to 5×10^8 cycles for nonferrous materials. Even though the stress induced is small enough to be elastic in nature, plastic deformation can occur at the tip of the crack. Data of high-cycle fatigue is typically represented by a plot of stress, S , versus the number of cycles to failure, N . The value of stress can be σ_{max} , σ_{min} or σ_a which are maximum stress, minimum stress and the stress amplitude respectively. The S-N relationship is generally established for a particular magnitude of the mean stress, σ_m , or one of the two ratios, R or A.

Low Cycle Fatigue:

In low cycle fatigue, failure usually happens below 10^4 cycles. In low cycle fatigue, significant plastic deformation of the material occurs due to recurring localized yielding in the vicinity of stress raisers such as holes, fillets, and notches, despite elastic deformation occurring in the component macroscopically. In a typical low cycle fatigue test, uni-axial testing is done on smooth (un-notched) specimens under diverse cyclic deformation levels. In this case, strain control testing is performed instead of stress control testing and stress response throughout the test and cycles to failure are noted for these tests. Combining the equations proposed by Basquin and Coffin-Manson give rise to an equation that may be utilized in the estimation of the complete range of fatigue lives:

$$\frac{\Delta \epsilon}{2} = \frac{\Delta \epsilon_e}{2} + \frac{\Delta \epsilon_p}{2} \quad (\text{Equ. 2.6})$$

$$\frac{\Delta \epsilon}{2} = \frac{\sigma'_f}{E} (2N_f)^b + \epsilon'_f (2N_f)^c \quad (\text{Equ. 2.7})$$

where;

$$\frac{\Delta \epsilon}{2} = \text{Total strain amplitude}$$

$$\frac{\Delta \epsilon_e}{2} = \text{Elastic strain amplitude}$$

$$\frac{\Delta \epsilon_p}{2} = \text{Plastic strain amplitude}$$

$$\epsilon'_f = \text{Fatigue ductility coefficient}$$

$$c = \text{Fatigue ductility exponent}$$

$$\sigma'_f = \text{Fatigue strength coefficient}$$

$$b = \text{Fatigue strength exponent}$$

$$E = \text{Modulus of elasticity}$$

$$2N_f = \text{No: of reversals to failure}$$

2.2 HISTORIC OVERVIEW OF FATIGUE:

Even today, fatigue failure is understood only up to a certain extent. What is known till now through researchers in a step-by-step approach has also become quite complicated. A succinct historic review of research works pertinent to metal fatigue is presented here to show how knowledge evolved by the hard work of several researchers/engineers. It was initially identified in 1840s that repeated stresses were the root cause for the major engineering damages in railway industry. Failures were commonly observed at shoulders of railroad axles even after the sharp corners were eliminated. As these failures seemed to be dissimilar from usual ruptures related with monotonic testing, the flawed theory of “crystallization” because of vibration was projected but was refuted later on. The term “fatigue” was coined in between 1840s and 1850s to portray failures taking place from repeating stresses. Between 1850s and 1860s, August Wohler of Germany carried out several laboratory fatigue tests that were pertinent to the failures of railway axle and that work is viewed as the first organized examination on fatigue. Wohler is hence named as the “father of systematic fatigue testing”. By means of stress (vs) life (S-N) diagrams, Wohler showed that fatigue life reduced at higher amplitudes of stress and below a particular amplitude of stress, the test specimens never failed. Wohler thus proposed the concepts of fatigue limit and S-N diagram. He proved that the range of stress is more vital than the maximum stress in case of fatigue. Between 1870s and 1890s, several engineers/researchers validated and extended Wohler’s classic work. The influence of mean stress was examined by Gerber and others, while a simplified theory pertaining to mean stresses was presented by Goodman. Their names are even today mentioned with diagrams concerned with alternating and mean stresses. In 1886 Bauschinger showed that the yield strength either in tension or compression decreased after the application of load of opposite sign that instigated inelastic deformation. This classic finding was the first indicator for the fact that even one reversal of inelastic strain can change the stress strain behaviour of metals. It was the first attempt to understand the concepts of cyclic hardening and softening of metals. In the beginning of 20th century, Ewing and Humfrey used optical microscope to study the mechanism of fatigue and localized slip bands and slip lines which lead to the creation of micro-cracks were observed. In 1910, Basquin depicted that the (S-N) alternating stress (vs) number of cycles to failure curves in the finite life region could be represented as a log-log linear relationship. Basquin’s equation with some amendments is even today used to indicate finite life fatigue behaviour. Gough and others, in 1920s contributed significantly

to understand fatigue mechanism. They further did the combinatorial analysis of bending and torsion (multi-axial fatigue) and a book on fatigue of metals was published by Gough in 1924. In 1927, Moore and Koppers published the first American book on metal fatigue. In 1920, Griffith published his research work on brittle fracture of glass and concluded that the strength was dependent on the dimensions of microscopic cracks. The relation $S\sqrt{a} = \text{constant}$ was introduced where 'S' is the nominal stress at fracture and 'a' is the crack size at fracture. With this exemplary effort on the significance of cracks, the base for fracture mechanics was created and Griffith is hence considered as "early father" of fracture mechanics. In 1924, Palmgren proposed a cumulative damage model for ball bearing design under variable amplitude loading. In 1920s, McAdam undertook rigorous corrosion fatigue studies where he depicted large reduction of fatigue life in various water solutions. The reduction was profoundly noticeable in high strength steels. In 1930, Haigh presented a lucid elucidation about the variations in the response to fatigue loading in the presence of notches by comparing high tensile strength steel and mild steel. As part of the work, notch strain and residual stress analysis were used that were further developed by others in later point of time. In 1930s, a significant advancement to improve fatigue strength was attained in the automobile industry by using shot-peening. Springs and axles, which were common candidates for fatigue failure, thereafter failed rarely. Almen elucidated a remarkable fatigue strength improvement in peened parts due to residual stresses of compressive nature being induced in their surface layers. This work became popular and the usage of peening/ other methods that can induce beneficial compressive residual stresses was promoted in the industry across the globe. Horger further proved that the growth of cracks could be prevented by surface rolling. Neuber, in 1937 presented the effect of stress gradient at notches and the well-liked elementary block concept. His theory states that the average stress over the tiny volume at the notch root is of more importance than the maximum stress at the notch. In 1939, Gassner highlighted the significance of conducting variable amplitude fatigue tests and proposed the utilization of a block loading spectrum of eight steps for simulation testing. Block testing was popular till 1950s and early 1960s i.e., the time when closed-loop electro hydraulic fatigue test equipment were available. During the World War II purposeful usage of residual stresses compressive in nature became widespread in aircraft engines and armoured vehicles design process. Numerous brittle fractures in Liberty ships and welded tankers forced engineers and researchers to think regarding pre-existing cracks and the effect of stress concentrations on the life. Many of the brittle fractures initiated at

the square hatch corners and welds. Solutions proposed to this problem were rounding the corners, adding riveted crack arresters, and giving more prominence to the material properties. In 1945, Miner extended the Palmgren's linear cumulative fatigue damage criterion of 1924. That is now familiar to engineering community as "Palmgren-Miner linear damage rule". It is used popularly in fatigue design process and, even with its several shortcomings, sustains as a vital means in prediction of fatigue life. In 1946, the formation of ASTM Committee E-09 on Fatigue opened the doors for development in fatigue testing standards and research. Peterson who was the first chairman of the committee proposed the fatigue notch factor (K_f) to be a function of the theoretical stress concentration factor (K_c), the geometry of notch and that of the component, and the UTS of the material. He wrote a book about stress concentration factors in 1953 and a revised version of that book was also published in 1974. Comet was the first commercial jet-propelled airplane and it started operations in May 1952 subsequent to flight tests of more than 300 hours. In January 1954, four days after a regular service check it slammed into the Mediterranean Sea. After the accident, the wreckage possible was recovered and a detailed study on components of the airplane was conducted and it was finally concluded that the disaster happened due to the fatigue failure in the cabin. Cracks of small size started from the corner of a fuselage opening. Post this incident; the fail-safe design started becoming a popular replacement for safe-life design in USA for aircrafts. This highlighted the necessity for much more emphasis on inspection and maintenance as thorough inspection and proper maintenance can save several lives.¹² Most important breakthrough in the field of fatigue investigations in 1950s was the arrival of close loop servo-hydraulic test machines that enabled improved load history replication on specimens and components. Scanning electron microscopy opened doors to a better understand the mechanism of fatigue. Irwin presented a stress intensity factor K_I that was recognized as the foundation for linear elastic fracture mechanics (LEFM) and coined the term "fracture mechanics". Due to his great contributions to the field, he is called the modern "father of fracture mechanics". In 1960s, low-cycle strain-controlled fatigue analysis started becoming popular by introduction of a relation between plastic strain amplitude and fatigue life. The relation was proposed by Manson and Coffin and it was endorsed by Topper and Morrow. The Neuber's rule and rainflow counting by Matsuishi and Endo in 1968 are the basis for today's notch strain analysis for fatigue. Establishment of the "Special Committee on Fracture Testing of High-Strength Steels" in 1960s by ASTM was the foundation for the creation of "ASTM Committee E-24 on Fracture Testing" in 1964. Lot of contribution was done by the committee in the areas of fracture mechanics and

fatigue crack growth. In 1993, this committee was merged with Committee E-09 of ASTM to form the “ASTM Committee E-08 on Fatigue and Fracture”. In 1960s, Paris presented that the rate of crack growth due to fatigue, da/dN can be better described by using the stress intensity factor range ΔKI . In 1960s, the disastrous crash of the aircraft F-111 was due to brittle fracture of the components that were having pre-existing flaws. During the B-1 bomber development program of 1970s, all the previous aircraft fatigue failures till date were taken into consideration and it was decided to use fracture mechanics concepts. This program was grounded on analysis of a detectable initial crack of known size. The Point Pleasant Bridge, West Virginia, USA, collapsed with no prior indication in 1967. Deep study exposed the fact that a fracture in an eye bar due to the growth of a crack to a critical size was the root cause for the failure. The preliminary defect was because of fatigue, corrosion fatigue and/or stress corrosion cracking. This collapse had a great impact on succeeding design standards proposed by the „American Association of State Highway and Transportation Officials“. Elber, in 1970 proposed a quantitative model which proved that fatigue crack growth was governed by an „effective stress intensity factor range“ and not the13 „applied stress intensity factor range“. This theory was called the „Crack Closure Model“ and it is popularly used even today. In the same year, Paris established that a stress intensity factor called the „threshold stress intensity factor“ can be attained for which growth of fatigue crack would not happen. In July 1974, the Air Force of United States of America issued MIL A-83444 related to the design of new military aircrafts, where damage tolerance requirements were described comprehensively. The usage of fracture mechanics concepts in fatigue analysis was systematically implemented by practice and regulations. The augmented necessity for an enhanced quantitative, non-destructive testing capability as a part of damage tolerance requirements was also highlighted. In 1980s and 1990s, many investigators explored the complicated problem of multi-axial fatigue. Brown and Miller proposed a critical plane method which inspired several researchers and that led to the development of many critical plane models. Emphasis on the fatigue analysis of materials used in electronics industry increased to a greater extent, together with considerable research work on thermo-mechanical fatigue. Polymer, metal, and ceramic matrices based composite materials were fabricated for several diverse applications. Great advancements were attained in polymer and metal matrix composites. The advances in aerospace and allied industries encouraged these achievements in composite materials, primarily. During that period, several complicated and costly aircraft parts designed by using safe-life design were regularly being retired for additional safety requirements and reasons. From the stand point

of fatigue design this needed deep analysis and the use of non-destructive testing and fracture mechanics. The deadly accident of Boeing 737 in 1988, subsequent to more than 90,000 flights, created a great need for improved maintenance and non-destructive inspection. Corrosion and/or fatigue and inadequate testing were the major contributors to the multisite damage (MSD) problems that occurred in several airplanes. In-depth studies were undertaken to appreciate and resolve the issue. In 1980s and 1990s, several modifications happened in fatigue design due to the advancements in computers and allied technologies. Software packages were developed for various fatigue life models and several advances were introduced in the packages to embed in the capability to simulate real time loading conditions like variable amplitude conditions etc. This almost made field testing possible in the laboratory. Improved digital prototyping with a smaller amount of testing is the 14-primary goal of fatigue design of twenty-first-century. Current day finite element software packages like ANSYS, ABAQUS etc. have capability to simulate complex boundary conditions that exist in real time. They also provide facility to conduct the fatigue analysis on the actual component geometry through simulation instead of a specimen with standard dimensions as in the case of experimentation. Thus, the results are sometimes more accurate with simulation when compared to experimental runs on the fatigue testing machine. The software packages are still being improved continuously to replace more and more physical testing.

2.3 EFFECT OF NOTCH ON THE FATIGUE LIFE OF STEELS

In case of pointed notches, the „notch sensitivity“ K_f/K_t raises along with the notch size. For as-received steels, the notch sensitivity is much superior at a stress ratio $R = -1$ when compared to $R = 0$. This means that, at $R = -1$, the as-received steels are less sensitive to notches compared to the heat-treated counterparts. For a given notch size, tempering temperature does not have considerable influence on notch sensitivity in the case of heat-treated steels. Further, notch sensitivity and ductility from true fracture strain cannot be related through any direct relation. M. Makkonen et. al. studied the fatigue performance of tempered steel specimens with grooves and came to a conclusion that a single method cannot be used alone to estimate the endurance limits of sharp notches and blunt notches. In the case of very sharp notches, the plastic strain even at the endurance limit was substantial, and that should be accounted for. In case of blunt notches where the plastic strain was insignificant, endurance limit was precisely estimated with the blend of statistical and geometric size effects. The statistical size effect itself provided sufficiently precise answers

for engineering purposes. Fatigue limit of sharp notches should be approximated by a technique that considers the fact that, as the notch's radius of root reduces, the fatigue/endurance limit moves towards a value that is attained as follows.

- Assume notch to be a pre-existing crack.
- Crack depth is equivalent to notch depth.
- Fatigue limit will be computed for the crack through “linear elastic fracture mechanics” and the “stress intensity factor range threshold”.

The effect of notch geometry on the fatigue life of HS and LS steels was explored by G.H. Majzoubi et. al. and it was found that notch geometry has high impact on a material's fatigue life. In high strength steels, the reduction was around 50%, while in low strength steels; the reduction depended on fatigue life and ranged from 20% to 75% for low-cycle fatigue tests to high-cycle fatigue tests. V-shape notches were the most harmful ones to the fatigue life of a member when compared to rectangular and U-shape notches. Maximum reduction in fatigue life was observed for V-shape notches while a minimum fatigue life reduction was observed in the case of U-shape notches.

From the results of the experimental runs performed by N. Mamidi et. al. on Rotary Bending Fatigue Testing Machine, it was enunciated that the depth of notch had high impact on the reduction of fatigue life of steels. The reduction of fatigue life was insignificant till a threshold depth, but as the depth of notch reached around 25% of the total diameter of the specimen, there was a drastic reduction.

2.4 FATIGUE LIFE PREDICTION METHODS

Fatigue failure of a structural member generally comprises the three stages of “crack initiation”, “crack propagation” and “final fracture”. This is a very much confined process and hence the local parameters of material, geometry, and loading have a profound effect on the fatigue life. They ought to be maintained as near to actuality as possible while undertaking fatigue life evaluation and particularly so when trying to improve the fatigue life/resistance. Standard guidelines for design of fatigue resistant structures, no doubt take local effects into account, but only approximately. They are mostly grounded on “nominal stress approach” that is a global standard and are accompanied by other general design guidelines. These guidelines-based approaches may not always be suitable, especially in

places where members undergo complex/variable amplitude loads with substantial number of cycles or where quantifying the nominal stresses cannot be done directly/ easily. Local methods which are based on local stress/strain values should be applied here. Local strain measurement can be done using strain gauges, and local stress computations are mainly done using F.E. method. Design engineers need sound techniques for assessing the values of local stresses and strains which thereby are used to compute the fatigue life of members. But these requirements generally can be met only insufficiently in real time. There are multiple methods available to predict the fatigue life of structural members on the basis of local parameters and they are complex to summarize and assess. Several researchers, engineering professionals and national agencies prefer multiple approaches to predict fatigue life as all methods are insufficient if used alone with respect to user demands. Further, the local parameter data do not have statistical proof and hence the usage of local methods lags behind when compared to the facilities provided by computerized fatigue analysis.

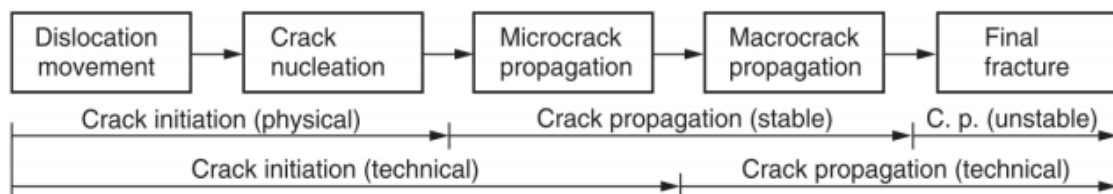


Figure 2.2: Phases in fatigue failure

If the surface length of the crack attains values which can be found by common technical approaches, then a technical crack is considered to have begun. The common acceptable dimensions are 1 mm of length and 0.5 mm of depth. Evaluation of fatigue strength is performed in two methods; 1. To find fatigue strength at a pre-set number of cycles. 2. To find specimen/component life for given load values. The global methods utilize crucial values of loads/nominal stresses that are associated to “global phenomena”, such as full plastic yield or complete fracture/ breakage of the coupon. Strength evaluations are named as “local approaches” if they are based on “local stresses or local strains”. Local methods of damage due to fatigue are taken into account, i.e., initiation of crack, propagation of crack and the final fracture. Crack initiation can be analysed by “notch-stress approach” or “notch strain approach” which are based on strains/stresses at the root of notch. Crack propagation and final fracture are illustrated by “crack propagation approach” which ensues from a pre-existing initial crack. An approach that acts as a link amid the global and local methods is the “structural stress approach”. In case of welded joints, several peculiarities are inherently

present that make the implementation of local approaches difficult for fatigue life prediction. These peculiarities can be welding defects, inhomogeneous material existence in the weld, distortions, residual stresses in the weld and other geometric weld characteristics. They are generally insignificant in the local approaches. Generally, the properties of the base material are taken for the analysis and the residual stresses are also approximately evaluated. Geometric weld constraints, imperfections and welding defects are separately considered in local approach based on an extreme scenario. Some of the popular methods for predicting fatigue life of welded joints as suggested by various researchers are; “Nominal stress approach for welded joints”, “Structural stress or strain approach for seam-welded joints”, “Notch stress approach for seam-welded joints”, “Notch strain approach for seam-welded joints”, “Crack propagation approach for seam-welded joints”, “Notch stress intensity approach for seam-welded joints”, “Local approaches applied to a seam-welded tubular joint”, “Structural stress or strain approach for spot-welded and similar lap joints”, “Stress intensity approach for spot-welded and similar lap joints” and the “Notch- and crack based approaches for spot-welded and similar lap joints”. A novel mathematical fatigue life evaluation model was developed by V. Balasubramanian et. al. for arc welded cruciform joints consisting of lack of penetration defect. The base material taken up for the investigation was ASTM 517 “F” Grade steel i.e., quenched, high strength, and tempered steel. The model was built based on “Response Surface Method” (RSM) and its validity was checked by applying Analysis of Variance (ANOVA) technique. The impact on the fatigue life due to joint dimensions was investigated in detail and it was concluded that the new model proposed could predict the fatigue life of “Shielded metal arc welded cruciform joints containing LOP defects” with 99% confidence level. The impact of cruciform joint dimensions on fatigue life was also examined as part of the research and it was found that straight profile fillet welds, large weld sizes and small LOP sizes showcased superior fatigue lives compared to other weld combinations. Several statistical fatigue life models based on an S-N approach were developed for fillet-welded steel joints where cracks originate from the weld toe. These models in principle consider that the number of cycles N to failure is directly related to the applied nominal stress range ΔS . They also presume that a fatigue limit exists and it is a stress range below which no fatigue failure takes place. Substantial fatigue life scatter is displayed, even for constant amplitude loading under controlled laboratory circumstances. This makes the usage of statistical methods inevitable and fatigue life is generally predicted for a particular confidence level under pre-defined loading conditions and environment. The commonly used method is, assuming that vital parameter

for fatigue life is the „nominal applied stress range“, and other loading parameters such as the „mean stress“ have insignificant effect for as-welded joints. The relation between number of cycles and stress range is decided by constant amplitude load tests at various stress range levels. A novel total life approach was proposed by S. Mikheevskiy et. al. which yielded a satisfactory assessment of the fatigue life for welded A-36 steel T-Joint configurations. The model made use of the “total life fatigue crack growth analysis technique” for loading histories of constant and variable amplitude and allowed calculating the fatigue life of a member with no requirement of splitting up the fatigue phenomenon into the „crack initiation“ and “crack propagation“ stages. T-joint specimens were analysed for two distribution types of residual stress:

- a) the as measured actual stress and
- b) the equilibrated modified stress.

There was only a minor variation between fatigue lives predicted through both the approaches. Examination of residual stress field for all welded joints experimentally becomes an expensive and time-consuming affair. Hence, the usage of standard residual stress fields available for various types of weld geometries was suggested. For welded structures, a fatigue life prediction system has been designed by Teppei Okawa et. al., in which minor initial cracks are presumed to form along the toe of a weld bead, and their growth and coalescence performance, was simulated up to the time when a crack breaks through the plate thickness, which represented the fatigue life. By applying a strip yield model, the simulation of crack opening/closing behaviour makes it probable to sufficiently analyse the propagation of fatigue cracks by considering the impact of loading sequence and the residual stress. The developed system proved competent for analyzing the fatigue life of welded joints, and the prediction outcomes agreed well with those acquired with definite fatigue tests. This system is likely to find wide range of uses in the fields of fatigue design and 21 maintenances for ships, construction machinery, plants, bridges, and other welded structures as a way for improving their reliability, reducing environmental loads and extending their service life.

2.5 FATIGUE ANALYSIS USING FINITE ELEMENT METHOD:

Typically weld seams constitute a small part of large assemblies and hence to perform fatigue analysis of welded joints large structures need to be analysed. Finite element models

created from the overall structure are not appropriate for fatigue studies that are grounded on the local stress/strain rates. The model of the global structure can be utilized to discover hot spots and also to transfer the loads applied to local deformations. International Institute of Welding and other organizations call for a very inclusive and explicit representation of the welded joints for analysis purpose. ANSYS Workbench pre-processing capabilities when combined with ANSYS sub modelling technology can prove to be a rapid and reliable solution. ANSYS Workbench Fatigue Tool is an efficient way to find the fatigue life of large welded assemblies. Amalgamation of Workbench's geometry/meshing capabilities, effective notch stress concept and the ANSYS Sub-modelling algorithm can give rise to a rapid, reliable, robust and accurate means for fatigue analysis of large three-dimensional structure. nCodeDesignLife which is an up-front design tool offers different time-tested methods for fatigue analysis of seam-welded structures. The tool permits fatigue calculations to be done as per the existing standards like ASME, BS7608, Eurocode 3 or by means of the "Volvo" approach. Analysis can also be performed using shell or solid element models by utilizing standard, generic or user defined S-N curves. The tool further takes into consideration, the impact of loading type, sheet thickness, mean stresses and small cycles. The tool can also be appropriately used for a wide range of sheet thicknesses and these techniques are all available in nCodeDesignLife's process-oriented user interface.

An FE-based method has been established and evaluated for numerically predicting fatigue lives of MAG-welded thin-sheet structures. The technique works well for the load cases analysed in this work. It is established to give functional outcomes at crucial locations, such as weld starts and weld corners, without the need for element-intensive refinements. Investigation results from 8 different welded steel specimens have been used to validate the method. It was observed that there is a strong connection between the slope of the S-N curve and the bending moment along the weld line. All test outcomes could be fitted to 2 different curves. The S-N curves are set up for sheet thicknesses between 1–3mm. This period does not seem to need any balancing factor for sheet thickness. Nevertheless, this may have to be scrutinized further for thicknesses outside this interval. A ratio, r , defining the ratio of bending stress over total structural stress is introduced, and used for picking suitable S-N curve. Welded joints of the studied type are often made in aluminium. The planned method for fatigue-life prediction should also be applicable for other materials than steel

2.6 STAINLESS STEELS

Stainless steels are low carbon alloy steels with chromium as a key alloying element. The corrosion resistance of steels is due to the existence of substantial quantity of chromium that causes the creation of a skinny and strong layer of chromium-oxide, which protects the surface from corrosion. On the basis of their microstructure at room temperature, stainless steels are primarily divided into five groups.

Table 2.1: Classification of stainless steels	
Group	Salient Features
Ferritic stainless steels	<ul style="list-style-type: none"> • Contain 12 to 30% of Cr and small amounts of Mn and Si. • Cheaper than austenitic stainless steels. • Used in food & chemical industry vessels, heat exchangers, automobile parts etc.
Martensitic stainless steels	<ul style="list-style-type: none"> • Contains 12 to 18% of Cr and 0.12 to 1.2% of C. • Have good wear and abrasion resistance but less corrosion resistance than other stainless steels.
Austenitic stainless steels	<ul style="list-style-type: none"> • Ni also added as a major alloying element along with Cr. • Contains Ni is to expand the austenite range to room temperatures. • Possess good corrosion and heat resistant properties along with high ductility.
Duplex stainless steels	<ul style="list-style-type: none"> • Possess mix microstructure of austenite and ferrite that is possible by balancing the contents of Cr and Ni. • Similar to austenitic stainless steels, they possess higher strength and good ductility. • In addition, they have greater pitting corrosion resistance when compared to any other stainless steels.
Precipitation hardening stainless steels	<ul style="list-style-type: none"> • Provide optimum combination of the properties of martensitic (strength) and austenitic grades (corrosion resistance). • The higher tensile strengths of these steels are obtained through a heat treatment process. Hardening is obtained by the addition of elements like Cu, Al, Ti, Nb, and Mo. • These steels are popularly used in aerospace applications.

By varying the composition of alloying elements like C, Cr, Ni, Cu, Al, etc a particular microstructure can be obtained at room temperature. The microstructure influences the mechanical properties and corrosion resistance of stainless steels. Each group of the stainless steels have their advantages and limitations and form the most economical choice for a particular service condition.

CHAPTER 3: MATERIALS AND METHODS

3.1 MATERIAL USED: SUPER DUPLEX STAINLESS STEEL: -

Duplex stainless steels are a family of stainless steels. These are called duplex (or austenitic-ferritic) grades because their metallurgical structure consists of two phases, austenite (face-centered cubic lattice) and ferrite (body centered cubic lattice) in roughly equal proportions. They are designed to provide better corrosion resistance, particularly chloride stress corrosion and chloride pitting corrosion, and higher strength than standard austenitic stainless steels such as Type 304 or 316. The main differences in composition, when compared with an austenitic stainless steel is that the duplex steels have a higher chromium content, 20–28%; higher molybdenum, up to 5%; lower nickel, up to 9% and 0.05–0.50% nitrogen. Both the low nickel content and the high strength (enabling thinner sections to be used) give significant cost benefits. They are therefore used extensively in the offshore oil and gas industry for pipework systems, manifolds, risers, etc and in the petrochemical industry in the form of pipelines and pressure vessels. In addition to the improved corrosion resistance compared with the 300 series stainless steels duplex steels also have higher strength. For example, a Type 304 stainless steel has a 0.2% proof strength in the region of 280 N/mm², a 22%Cr duplex stainless steel a minimum 0.2% proof strength of some 450 N/mm² and a super duplex grade a minimum of 550 N/mm².

3.2 GRADES OF DUPLEX STEELS:

Duplex stainless steels are usually divided into three groups based on their pitting corrosion resistance, characterised by the pitting resistance equivalence number,

$$\text{PREN} = \%Cr + 3.3 \%Mo + 16 \%N.$$

3.2.1 Standard duplex (PREN range: 28–38)

Typically Grade EN 1.4462 (also called 2205). It is typical of the mid-range of properties and is perhaps the most used today

3.2.2 Super-duplex (PREN range: 38-45)

Typically grade EN 1.4410 up to so-called hyper duplex grades (PREN: >45) developed later to meet specific demands of the oil and gas as well as those of the chemical industries. They offer a superior corrosion resistance and strength but are more difficult to process because the higher contents of Cr, Ni, Mo, N and even W promote the formation of intermetallic phases, which reduce drastically the impact resistance of the steel. Faulty

processing will result in poor performance and users are advised to deal with reputable suppliers/processors. Applications include deep-water offshore oil production.

3.2.3 Lean duplex grades (PREN range: 22–27)

Typically grade EN 1.4362, have been developed more recently for less demanding applications, particularly in the building and construction industry. Their corrosion resistance is closer to that of the standard austenitic grade EN 1.4401 (with a plus on resistance to stress corrosion cracking) and their mechanical properties are higher. This can be a great advantage when strength is important. This is the case in bridges, pressure vessels or tie bars.

3.3 UNS S32760:

Material used in the current analysis is UNS S32760, Super duplex stainless steel. Its main uses are in the marine field due to its high pitting corrosion resistance. The composition varies slightly depending on the requirement.

Weight %	C	Si	Mn	S	P	Cr	Ni	Mo	N	Cu	W
Min.						24,00	6,00	3,00	0,20	0,50	0,50
Max.	0,030	1,00	1,00	0,010	0,030	26,00	8,00	4,00	0,30	1,00	1,00

3.3.1 CHARACTERISTICS:

- High resistance to stress corrosion cracking in halide containing environments.
- High resistance to pitting and crevice corrosion.
- High resistance to general corrosion.
- High mechanical strength.
- High resistance to erosion corrosion and corrosion fatigue.

3.3.2 MICROSTRUCTURE:

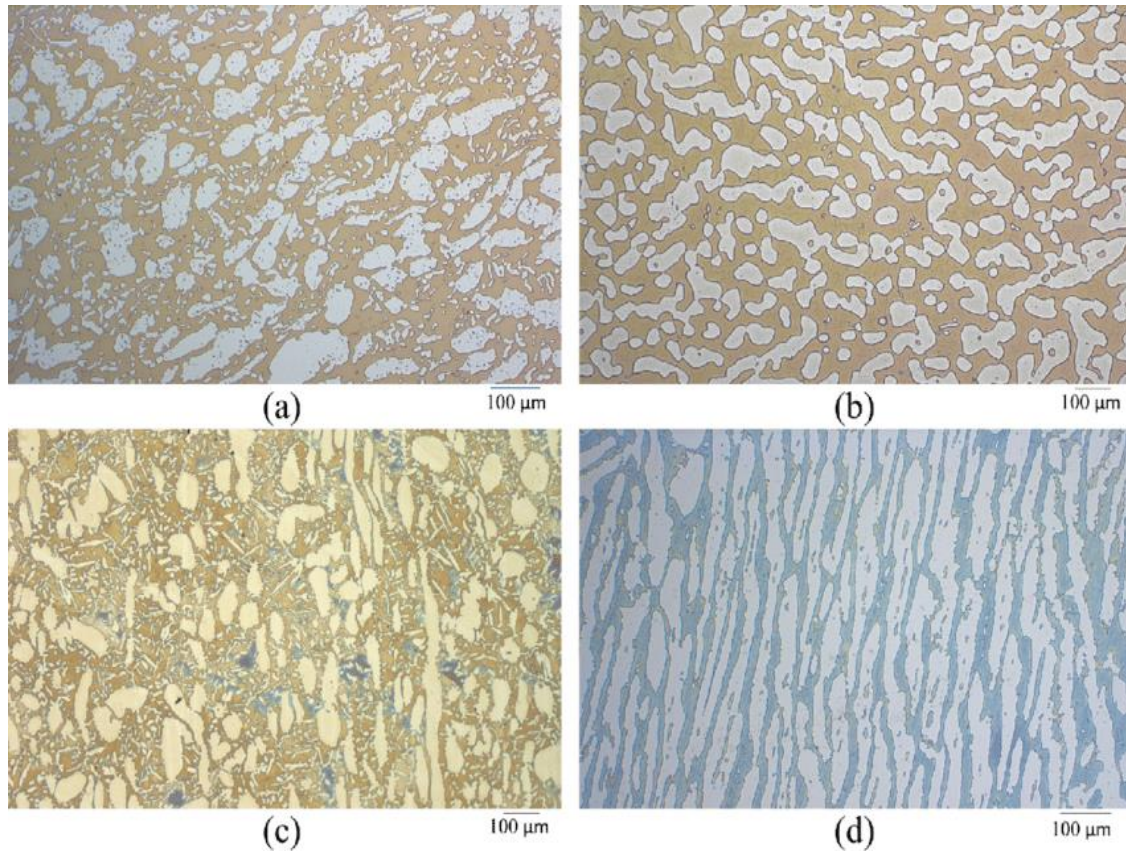


Fig 3.1 Light optical micrographs of (a) UNS S32750, (b) UNS S32760, (c) UNS S39274 extruded pipe, and (d) UNS S39274 rolled plate. The microstructure was revealed by applying two different etching steps. In the first step, a 15 wt.% KOH solution was used, and a potential of 3 V was applied for 12 s. In the second step, the solution was 20 wt.% NaOH with an applied potential of 1.5 V for 10 s

3.3.2 APPLICATIONS:

Architecture

Stockholm's waterfront building

Louvre Abu Dhabi

La Sagrada Familia

Infrastructure:

Helix Bridge, Singapore

Cala Galdana bridge

Hong Kong–Zhuhai–Macau bridge and undersea tunnel.

Sea walls, piers etc

Tunnels

Oil and Gas:

A wide range of equipment: flowlines, manifolds, risers, pumps, valves.

Pulp and Paper:

Digesters, pressure vessels, liquor tanks etc.

Chemical engineering:

Pressure vessels, heat exchangers, condensers, distillation columns, agitators, marine chemical tankers etc.

Water:

Desalination plants, large tanks for water storage, waste water treatment

Renewable energy: Biogas tanks

Mobility:

Tramcars and bus frames, tank trucks, iron ore wagons

Engineering:

Pumps, valves, fittings, springs, etc.

3.4 METHODS:

3.4.1 STRAIN BASED FATIGUE LIFE ESTIMATION

Through ϵ -N method, the strain range $\Delta\epsilon$ at critical location and its initiation life (N) is related by “Coffin- Manson” expression introduced in 1910. Combining the equations proposed by Basquin and the Coffin-Manson give rise to an equation that may be utilized in the estimation of the complete range of fatigue lives.

$$\textit{Total Strain Amplitude}' = \textit{Elastic Strain Amplitude}' + \textit{Plastic Strain Amplitude}'$$

$$\frac{\Delta\varepsilon}{2} = \frac{\Delta\varepsilon_e}{2} + \frac{\Delta\varepsilon_p}{2}$$

$$\frac{\Delta\varepsilon}{2} = \frac{\sigma'_f}{E}(2N_f)^b + \varepsilon'_f(2N_f)^c$$

where,

$$\frac{\Delta\varepsilon}{2} = \text{Total strain amplitude}$$

$$\frac{\Delta\varepsilon_e}{2} = \text{Elastic strain amplitude}$$

$$\frac{\Delta\varepsilon_p}{2} = \text{Plastic strain amplitude}$$

$$\varepsilon'_f = \text{Fatigue ductility coefficient}$$

c = Fatigue ductility exponent

σ'_f = Fatigue strength coefficient

b = Fatigue strength exponent

E = Modulus of elasticity

$2N_f$ = No: of reversals to failure

Out of the different theories developed based on total strain amplitude, Muralidharan-Mansion method also called Modified Universal Slopes method is popularly used in predicting fatigue life of steels/ other alloys under different environment conditions.

$$\frac{\Delta\varepsilon}{2} = 0.623 \left(\frac{\sigma_u}{E}\right)^{0.832} (2N_f)^{-0.09} + 0.0196(\varepsilon_f)^{0.155} \left(\frac{\sigma_u}{E}\right)^{-0.53} (2N_f)^{-0.56}$$

3.4.2 TAGUCHI TECHNIQUE FOR NOTCH ANALYSIS:

The three factors chosen for Taguchi analysis of notch fatigue strength along with their high, medium and low levels are mentioned in 3.1. The experimental matrix given in Table 3.2 is a nine trial orthogonal array (OA) of Taguchi matrix i.e. L27. This OA provides complex

Factor	Notation	Units	Levels		
			Low	Medium	High
Width	w	mm	0.5	0.75	1
Depth	d	mm	0.5	0.75	1
Notch Central Angle	a	Degrees	120	240	360

enough array to demonstrate the amount of confounding that may occur in an experiment.

Table 3.2 Notch parameters for fatigue analysis

RUN	Coded values			Absolute Values		
	w	d	a	w	d	a
1	-1	-1	-1	0.5	0.5	120
2	-1	-1	0	0.5	0.5	240
3	-1	-1	1	0.5	0.5	360
4	-1	0	-1	0.5	0.75	120
5	-1	0	0	0.5	0.75	240
6	-1	0	1	0.5	0.75	360
7	-1	1	-1	0.5	1	120
8	-1	1	0	0.5	1	240
9	-1	1	1	0.5	1	360
10	0	-1	-1	0.75	0.5	120
11	0	-1	0	0.75	0.5	240
12	0	-1	1	0.75	0.5	360
13	0	0	-1	0.75	0.75	120
14	0	0	0	0.75	0.75	240
15	0	0	1	0.75	0.75	360
16	0	1	-1	0.75	1	120
17	0	1	0	0.75	1	240
18	0	1	1	0.75	1	360
19	1	-1	-1	1	0.5	120
20	1	-1	0	1	0.5	240
21	1	-1	1	1	0.5	360

22	1	0	-1	1	0.75	120
23	1	0	0	1	0.75	240
24	1	0	1	1	0.75	360
25	1	1	-1	1	1	120
26	1	1	0	1	1	240
27	1	1	1	1	1	360

CHAPTER 4: NUMERICAL METHODS

4.1 Prediction of Axial fatigue life from Tensile data

From a practical point of view, merely knowing that the elastic and plastic components are approximately straight lines is extremely useful because it means that only a few tests are needed to establish these lines. There are, however, many applications when it is desirable to avoid any fatigue testing whatsoever and to estimate these straight lines from a knowledge of more readily obtained material properties. Therefore, an attempt has been made to establish a correlation between these lines and the properties of materials obtained in simple tensile tests.

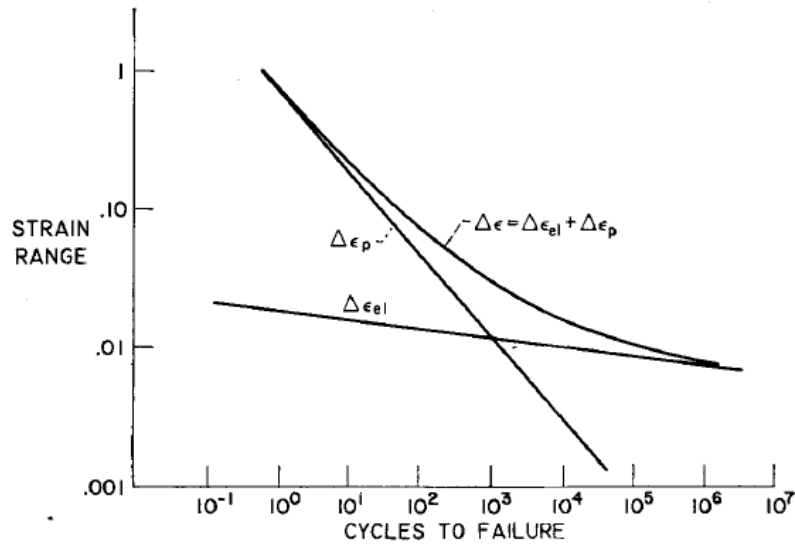


Fig 4.1 Strain range vs Cycles to failure

4.2 Four Point Correlation method:

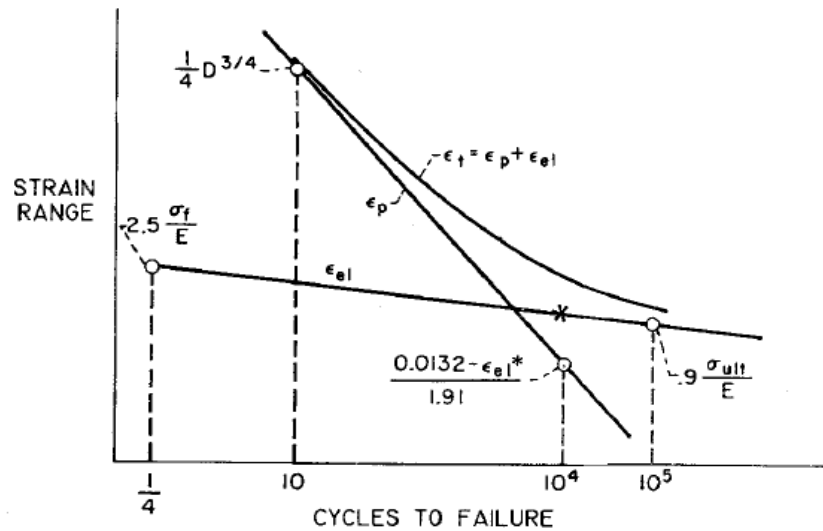


Fig 4.2 Strain range vs cycles to failure; Indicating the four points used in the aforementioned method

Figure shows one method of analysis that we have investigated. It may be referred to as a four-point correlation method because the two straight lines are obtained by locating two points on each of them. Every point is determined from a knowledge of the tensile behaviour of the material. A point is located on the elastic line at $1/4$ cycle with an ordinate $(2.5 \sigma_f)/E$, where σ_f is the true fracture stress of the material obtained by dividing the load at the time of failure in the tensile test by the actual area measured after failure has occurred. Another point on this line is obtained at 10^5 cycles. At this point, the ordinate is $(0.9 \sigma_u)/E$, where σ_u is the conventional ultimate tensile strength of the material. On the plastic line, a point at 10 cycles is determined that has an ordinate of $1/4D^{3/4}$, where D is the logarithmic ductility of the material defined as the natural logarithm of the original cross-sectional area of the specimen divided by the final cross-sectional area. The second point on the plastic line is obtained at 10^4 cycles as indicated in Figure. The point shown by the star at 10^4 cycles is first located on the elastic line and the ordinate observed. This ordinate is then substituted into the simple equation shown in the figure to obtain a corresponding ordinate value at 10^4 cycles for the plastic strain. This formula is derived from the observation that the plastic and the elastic strains at 10^4 cycles are approximately related to each other. The relation is almost (but not quite, see Ref. in RP) equivalent to the assumption that the total strain range at 10^4 cycles is approximately 1 percent for all materials. Thus, from a knowledge of the tensile properties, two points on each of the lines can be determined and the plastic and elastic components plotted as in Fig. 4.1. The curve of total strain range may be obtained by simple addition, as indicated by the curved line, which is asymptotic to the plastic line in the low-life range and to the elastic line in the high-life range. This curved line thus represents the estimated relation between total strain range and life for the material.

In order to obtain the fatigue properties in this way, the true fracture stress must be known; however, this property is not always given in the literature, and therefore an additional approximation is sometimes required. A very good approximation has been suggested by John O'Brien who, under contract with NASA, recommended that the fracture stress could be obtained by multiplying the ultimate tensile strength by the factor $(1 + D)$. Thus,

$$\sigma_f = \sigma_u (1 + D)$$

That this relation is valid is seen in Fig. a, where fracture stress is plotted against the product of $\sigma_u (1 + D)$. Each data point represents a different material, and the data generally fall close to a 45-deg line. By Using this approximation, only the elastic modulus and two tensile

properties, σ_u and reduction in area (which establishes D), are needed to predict axial fatigue life for a specified strain range. This is illustrated in Fig. 4.3. One simply locates the value of σ_u/E and the value of percent reduction in area on the horizontal axis, and then determines the intercepts at P1 and P4 from the dashed and solid families of curves. The location of points P2 and P3 are obtained from the auxiliary vertical and horizontal scales in the figure.

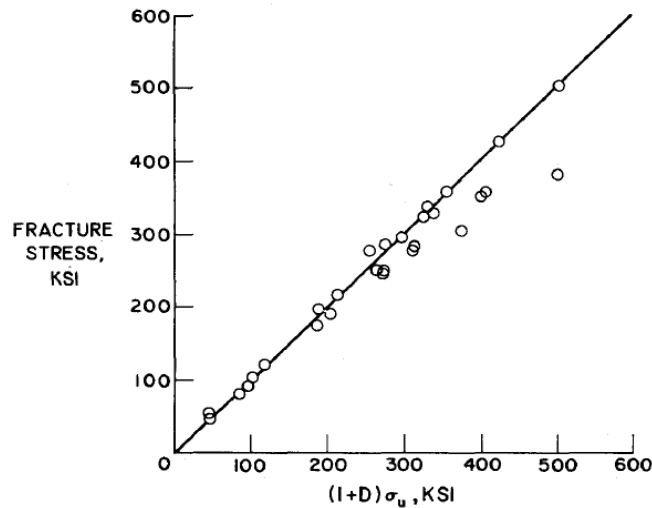


Fig 4.3 True fracture stress vs the approximation of John O'Brien

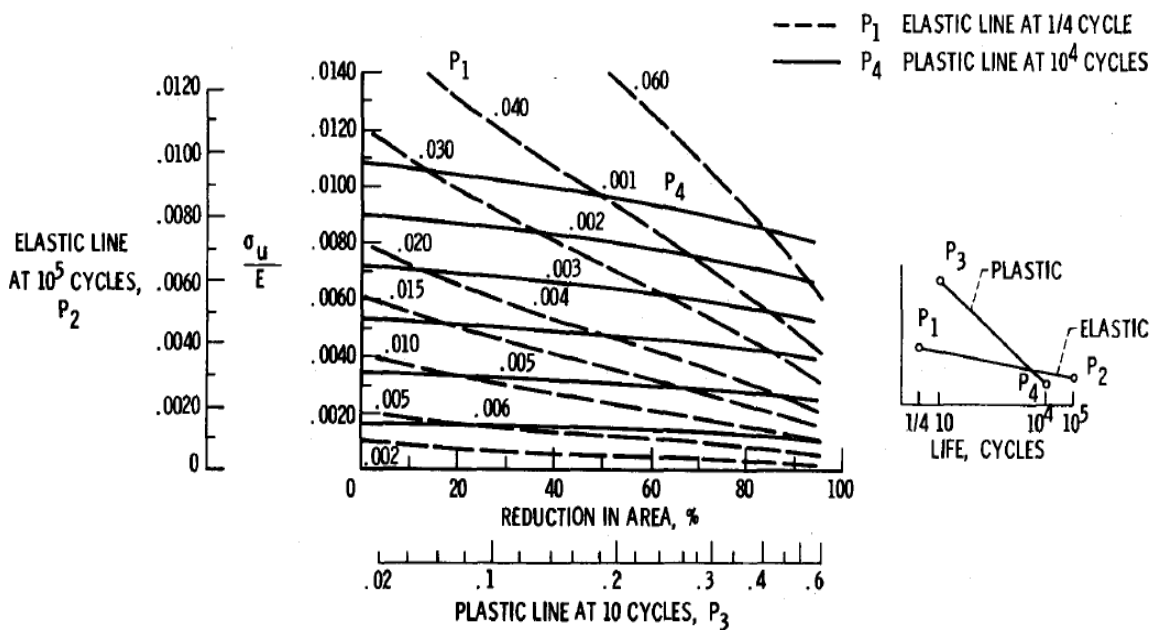


Fig 4.4 Ratio of UTS and E vs % reduction in area

The procedure described for determining the elastic and plastic lines was first developed by study of relatively few materials. Subsequently, the validity of this procedure was investigated by examining a larger number of materials. Those materials that have been studied in axial low-cycle fatigue tests to date are shown in Table 4.1. Alloys of nearly all

the important classes of structural materials are included. These materials cover quite a range in variables that might affect fatigue behaviour such as those shown in Table 4.2. Among them are crystalline structures wherein body-centered-cubic, face-centered- cubic, and hexagonal-close-packed arrangements are represented; reductions in area covering the range from 1 to 94 percent; tensile strengths from 16,000 to over 400,000 psi; high and low notch sensitivities; cyclic-hardening and -softening characteristics; high and low stacking-fault energy; etc. Thus, any conclusion that might be reached regarding the validity of the relations involving all of these materials cannot be regarded as being limited to a very small class of materials.

TABLE 1—MATERIALS FOR AXIAL LOW-FATIGUE INVESTIGATION

4130 Soft	Titanium 6Al-4V
4130 Hard	Titanium 5Al-2.5Sn
4130 X-hard	Magnesium AZ31B-F
4340 Annealed	Aluminum 1100
4340 Hard	Aluminum 5456 H311
304 Annealed	Aluminum 2014 T6
304 Hard	Aluminum 2024 T4
52100 Hard	Aluminum 7075 T6
52100 X-hard	Silver 0.99995 pure
AM 350 Annealed	Beryllium
AM 350 Hard	Inconel X
310 Stainless	A286 aged
Vascomax 300 CVM	A286 34 percent cold reduced and aged
Vascojet MA	D979
Vascojet 1000	

Table 4.1

TABLE 2—MATERIAL VARIABLES IN AXIAL LOW-CYCLE FATIGUE INVESTIGATION

Crystalline structure	Body-centered cubic Face-centered cubic Close-packed hexagonal
Methods of strengthening	Precipitation hardening Hot and cold worked
Reduction in area	1 to 94 percent
Tensile strength	16,000 to 411,000 psi
True fracture stress	48,000 to 500,000 psi
Elastic modulus	6.2×10^6 to 42.0×10^6 psi
Notch sensitivity	Notch ductile to very notch sensitive
Stacking-fault energy	Low (steels) to high (aluminum)
Cyclic behavior	Strain softening to strain hardening

Table 4.2

4.2.1 Modified Four-point correlation method:

To improve the original four-point correlation method, this method uses the four points PI'-P4' which provide better results, instead of the four points P1-P4 in Figure 4.4. The strain-life relation constants are given as

$$b = \frac{1}{6} \left\{ \log \left[0.16 \left(\frac{\sigma_u}{E} \right)^{0.81} \right] - \log \left(\frac{\sigma_f}{E} \right) \right\}$$

$$c = \frac{1}{4} \left[\log \left(\frac{0.00737 - \frac{\Delta \epsilon_e^*}{2}}{2.0274} - \log \epsilon_f \right) \right]$$

$$\frac{\Delta \epsilon_e^*}{2} = \frac{\sigma_f}{E} \left[10^{\frac{2}{3} \left(\log \left(0.16 \left(\frac{\sigma_u}{E} \right)^{0.81} \right) \right) - \left\{ \log \frac{\sigma_f}{E} \right\}} \right]$$

4.3 MURALIDHARAN AND MANSON METHOD:

The universal slopes equation developed by Manson and Hirschberg, is as given below

$$\Delta \epsilon = \left[\frac{N_f}{D} \right]^{-0.6} + 3.5 \frac{\sigma_u}{E} N_f^{-0.12}$$

where $\Delta \epsilon$ = total strain range
 N_f = fatigue life
 D = ductility
 σ_u = ultimate tensile strength

The slopes of the plastic and elastic lines were universalized as -0.6 and -0.12 for all materials. The accuracy of prediction by the Universal Slopes Equation has been quite remarkable, considering that only static properties are involved and that it has been applied to wide classes of materials. Recently, an effort was made to improve the equation given above based on the data of 47 materials under room temperature.

The following general equation was used as a starting point

$$\Delta \epsilon = A_1 D^{\alpha_1} \left[\frac{\sigma_u}{E} \right]^{\beta_1} N_f^{\gamma_1} + A_2 D^{\alpha_2} \left[\frac{\sigma_u}{E} \right]^{\beta_2} N_f^{\gamma_2}$$

Here the exponents (slopes of the lines on log-log coordinates) γ_1 and γ_2 are assumed constant for all materials. The coefficients are, however, generalized and allowed to be

power functions of both ductility D , ultimate tensile strength σ_u , and elastic modulus E for both the elastic and plastic components of the strain range.

The constants in the equation were found by optimization by the least squares approach using actual fatigue constants, as described in Fig. c, obtained from the experimental results on 47 materials taken from references, details of the mathematical procedure used for the determination of the constants can be found in the original paper. The Modified Universal Slopes Equation was determined to be:

$$\Delta\varepsilon = 0.0266D^{0.155} \left[\frac{\sigma_u}{E} \right]^{-0.53} N_f^{-0.56} + 1.17 \left[\frac{\sigma_u}{E} \right]^{0.832} N_f^{-0.09}$$

In the earlier equation, the exponent of D is 0.6, whereas, in the Modified Universal Slopes Equation, it is only 0.155. Further study on materials of unusual combinations of ductility and tensile strength would be interesting to clarify the conflicting implications of the two equations. It is also interesting that the more generalized analysis presented here and use of a larger number of materials provided little effect on the exponent of fatigue life for the plastic component but a large effect on the exponent of fatigue life for the elastic component. Thus, the universal slopes which were -0.6 and -0.12, have become 0.53 and -0.09, respectively. It has long been recognized that -0.12 was a rather steep slope to be used as an average for all materials. The value -0.09 is more typical of many materials examined since the first study. It also implies a lesser drop in life as extrapolations are made to life values much greater than 10⁶ cycles which should be satisfying to interested users in the very high cyclic life range.

4.4 ROESSLE AND FATEMI HARDNESS METHOD:

Roessle and Fatemi studied estimation method from Brinell hardness through the least square fitting analysis of the relationship between fatigue strength coefficient, σ'_f , and Brinell hardness, HB , parameters by using 69 pieces of fatigue test data. However, the relationship between fatigue ductility coefficient ε'_f and Brinell hardness is established through the intermediate variable of fatigue life, N_f . To determine the fatigue strength exponent, b , and fatigue ductility exponent, c , the statistical mean values of the 69 pieces of fatigue test data were taken as the approximation of the two exponents, respectively. The Hardness Method for fatigue properties estimation method was given as follows:

$$\sigma_f' = 4.25(\text{HB}) + 225$$

$$b = -0.09$$

$$\epsilon_f' = \frac{0.32(\text{HB})^2 - 487(\text{HB}) + 191000}{E}$$

$$c = -0.56$$

4.4.2 MODIFICATION BY SHAMSEI AND McLEVEY:

Based on the Hardness Method proposed by Roessle and Fatemi, a new fitting between fatigue strength coefficient, σ_f' , and Brinell hardness, HB , parameter is obtained:

$$\sigma_f' = 3.98(\text{HB}) + 284$$

When the Brinell hardness range is $150 < HB < 700$, ϵ_f' can be given as

$$\epsilon_f' = \frac{0.32(\text{HB})^2 - 487(\text{HB}) + 19100}{E}$$

The optimal segment fitting equation of fatigue ductility coefficient from Brinell hardness can be given as follows:

$$\epsilon_f' = 1.5 * 10^{-6} * (\text{HB})^{2.35} ; \text{HB} < 340$$

$$\epsilon_f' = 1.7 * 10^{-12} * (\text{HB})^{-4.78} ; 340 < \text{HB} < 700$$

4.5 MITCHELL'S METHOD:

Mitchell suggested that for steels with hardness below 500 BHN,

$$\sigma_f' = \sigma_u + 345 \text{ (MPa)}$$

$$b = -\frac{1}{6} \log \left[\frac{2(\sigma_u + 345)}{\sigma_u} \right]$$

$$c = -0.6$$

$$\varepsilon_f' = \varepsilon_f = \ln\left(\frac{100}{100 - RA}\right)$$

4.6 MEGGIOLARO AND CASTRO (MEDIAN) METHOD:

According to Meggiolaro and Castro, on average, steels present significantly higher b and c exponents than aluminium and titanium alloys. Therefore, different estimates for the Coffin–Manson parameters should be considered for each alloy family.

Correlations between Coffin–Manson’s exponents and the monotonic tensile test properties are poor. Even though the cyclic hardening exponent n_0 is well estimated by the ratio $b=c$ for steels, estimates for b and c based on n_0 are detrimental to all studied methods.

The relations given by the median method are as follows:

$$\sigma_f' = 1.5\sigma_u$$

$$\varepsilon_f' = 0.45$$

$$b = -0.09$$

$$c = -0.59$$

4.7 STRAIN LIFE PLOTS:

The strain amplitude percentage was calculated using all the above-mentioned methods and its values were varied with the fatigue life (or) no. of reversals which is simply obtained by multiplying the fatigue life by two. Such plots are called strain life plots and are important in strain-life fatigue analysis. These plots replace the S-N plots which are generally used in majority of the fatigue analyses. All the plots were compared and a method was chosen such that the fatigue life constants obtained conservative and close-to-actual results.

The plots obtained are as follows:

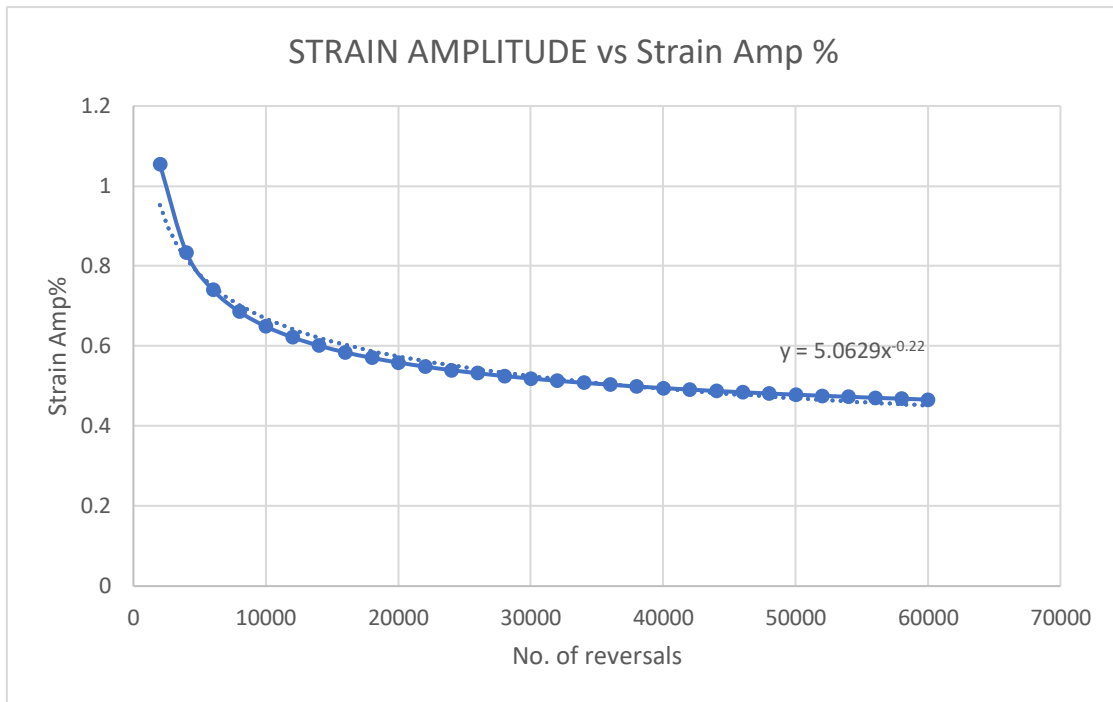


Fig 4.5 Strain life plot using Modified four-point correlation method.

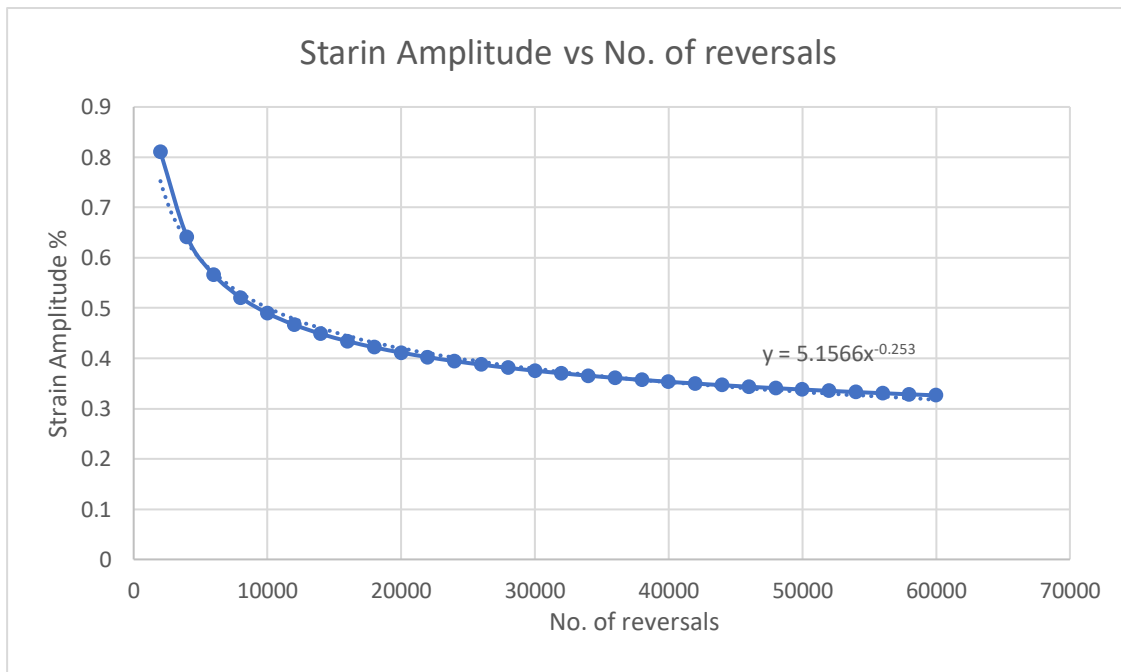


Fig 4.6 Strain life plot using Modified universal slopes method (Muralidharan and Manson method)

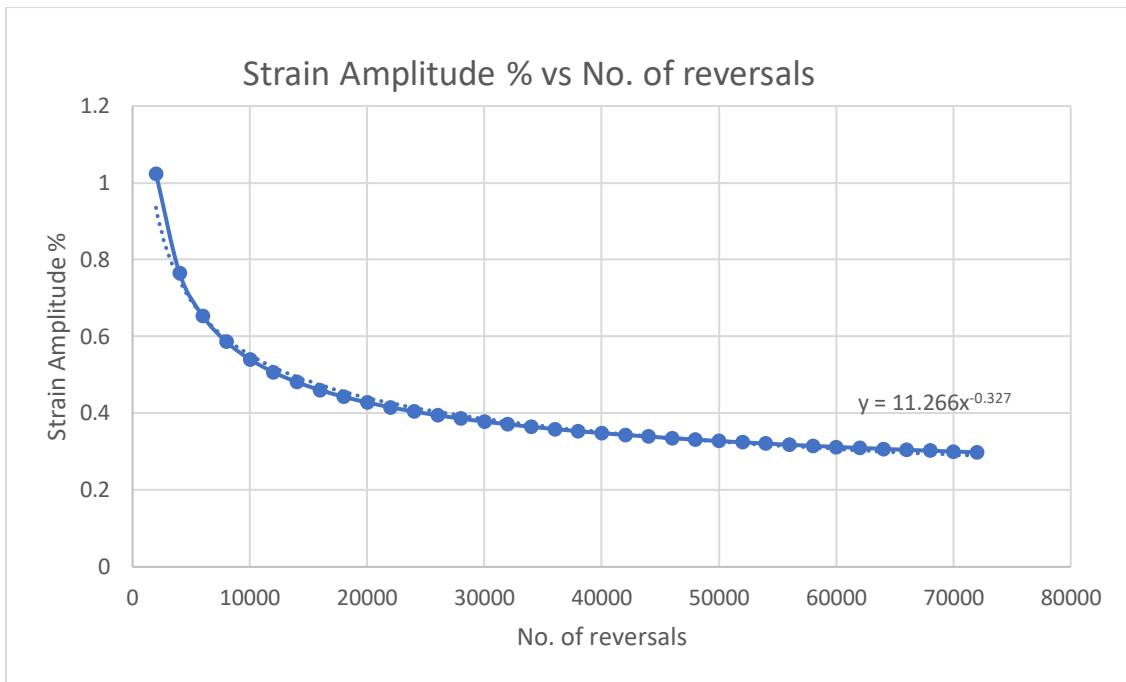


Fig 4.7 Strain life plot using Roessle and Fatemi Hardness method with modifications done by Shamsai and McLevey

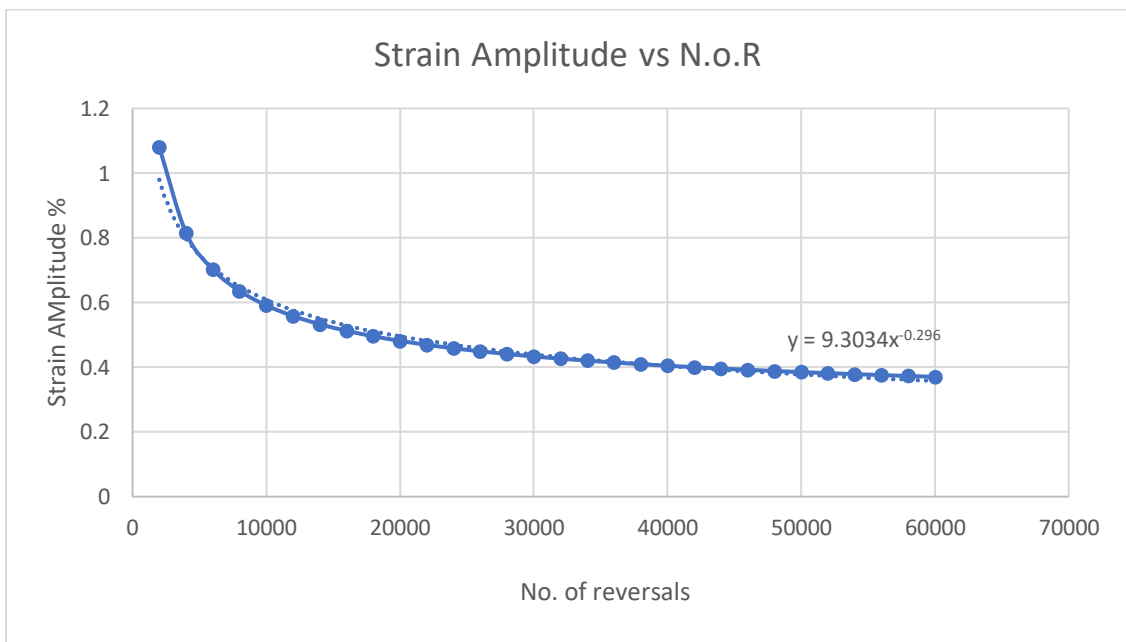


Fig 4.8 Strain life plot using Mitchell's method

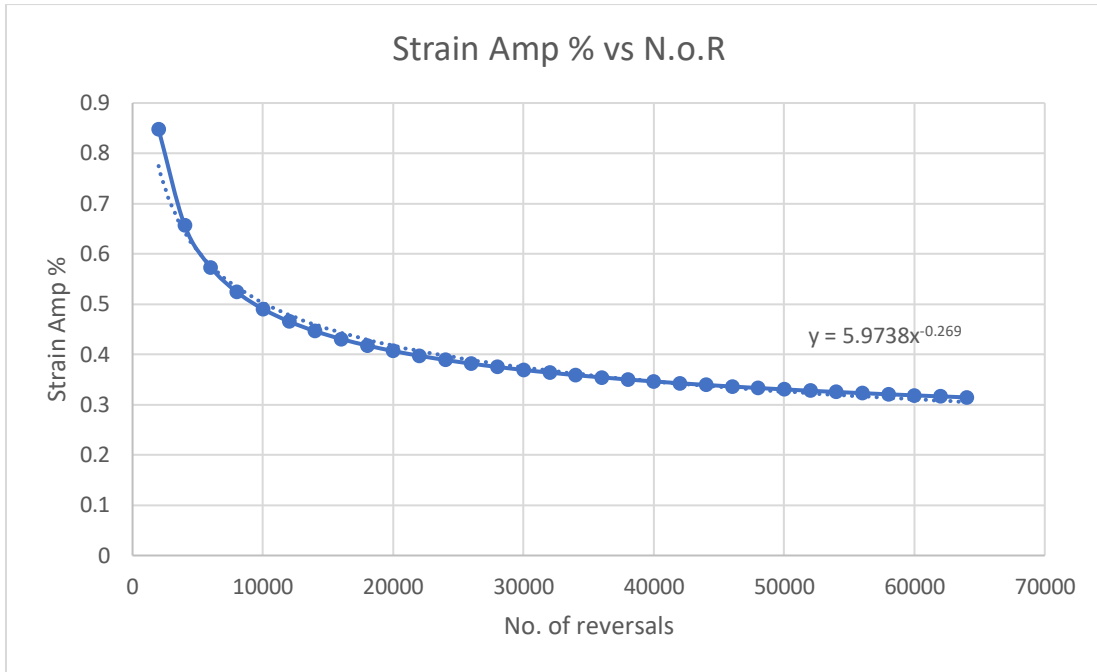


Fig 4.9 Strain life plot using Meggiolaro and Castro (median) method

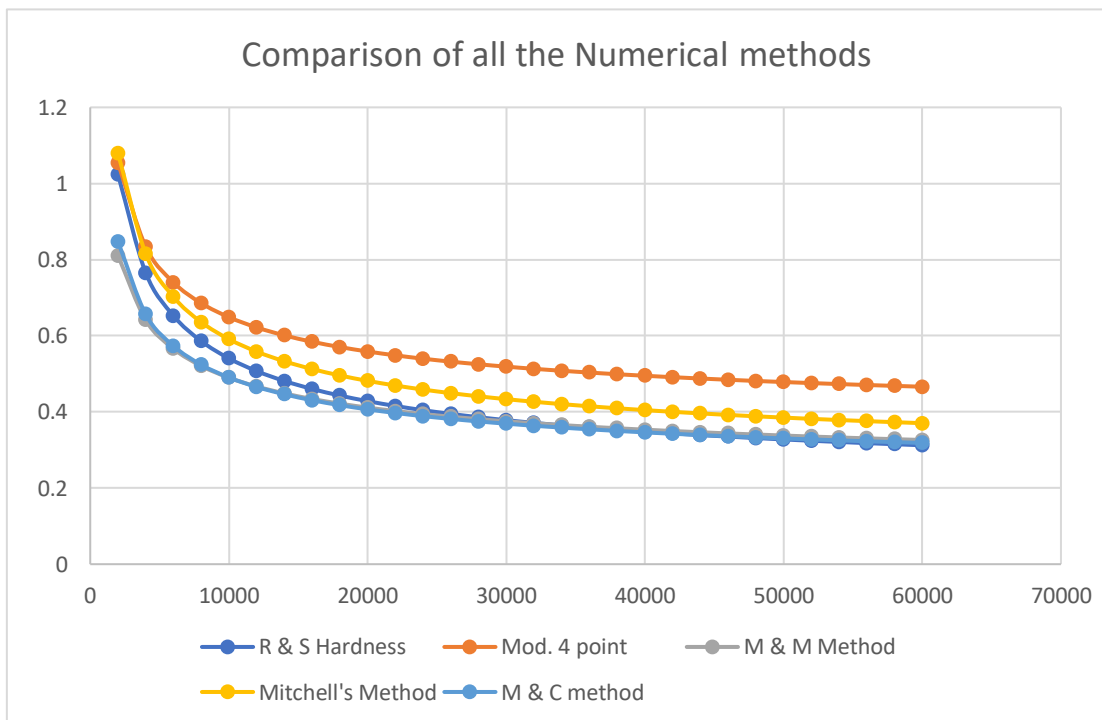


Fig 4.10 Comparison of Numerical methods

From the chart, it can be observed that all the methods predict the fatigue life constants which follow the same trend. Also, the Hardness method, Mitchell's method and Ong's modified four- point correlation method predict highly conservative values which are usually not recommended due to the over-utilization of material in design.

The Median method and modified universal slopes method predict almost same data values, only difference being the conservativeness of the Universal slopes method. Hence, the Muralidharan and Manson method is chosen to the method utilized in the current project. The wide usage of this method also is one of the reasons of consideration.

It must be pointed out that all the presented estimates should never be used in design, because for some materials, even the best methods may result in life prediction errors of an order of magnitude. The use of such estimates, even the proposed medians method, is only admissible during the first stages of design; otherwise, all fatigue properties should be experimentally obtained.

CHAPTER 5: FINITE ELEMENT METHOD

The fatigue tool available in ANSYS 2020 R2 was used to predict the fatigue life and maximum equivalent stress under load of super duplex stainless steel UNS S32760. The 3D model was created in FUSION 360 and imported to ANSYS as an IGES file

5.1 MESHING

Discretization was carried out using tetrahedron elements and a mesh refinement level of two. Along with the refinement, a fine span angle centering was utilized in meshing which spans an angle of 36-12 degrees for each element at the curved regions. Due to this curvature-based refinement, better approximation can be made compared to cases without this type of mesh sizing. The standard specimen (Fig 5.1) consisted of 19132 nodes and 9226 elements after being meshed with the above refinement and sizing applied.

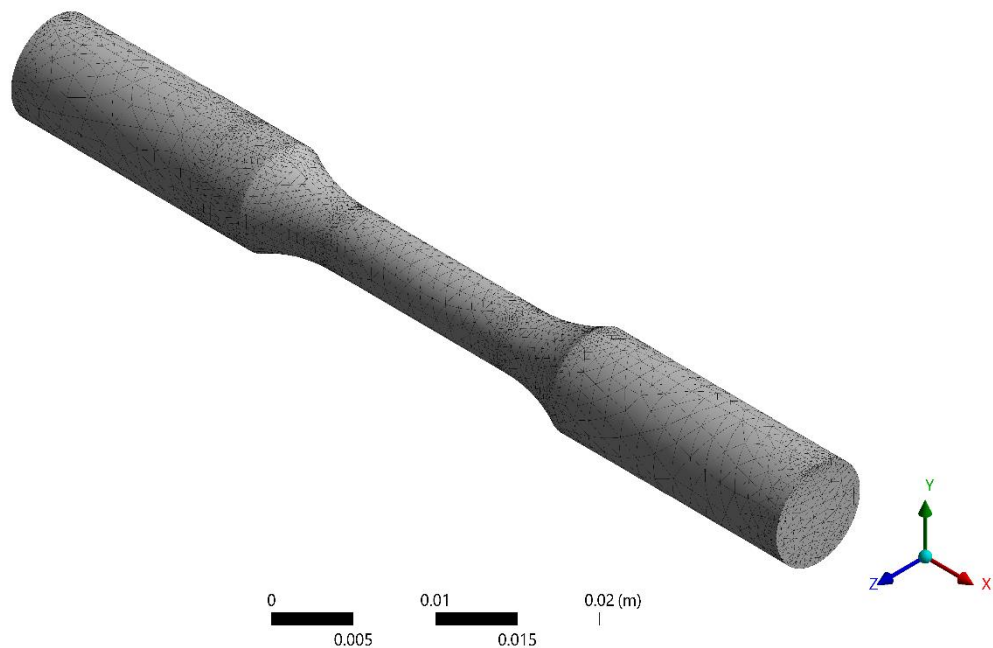


Fig 5.1 Standard fatigue test specimen 3D model with meshing

5.2 LOADING:

A fully reversed load was applied to all the specimen to predict the variation of fatigue life with different notch parameters. The load was applied at one end of the fatigue specimen with the other end fixed. The reversible load was then applied and fatigue life was approximated for each notch variant. The load was applied in the form of pressure with a

magnitude of 150 MPa and direction of x-axis. As the load is fully reversed in nature, max load on the specimen in a cycle is 150 MPa while the direction changes from negative-x to positive-x direction.

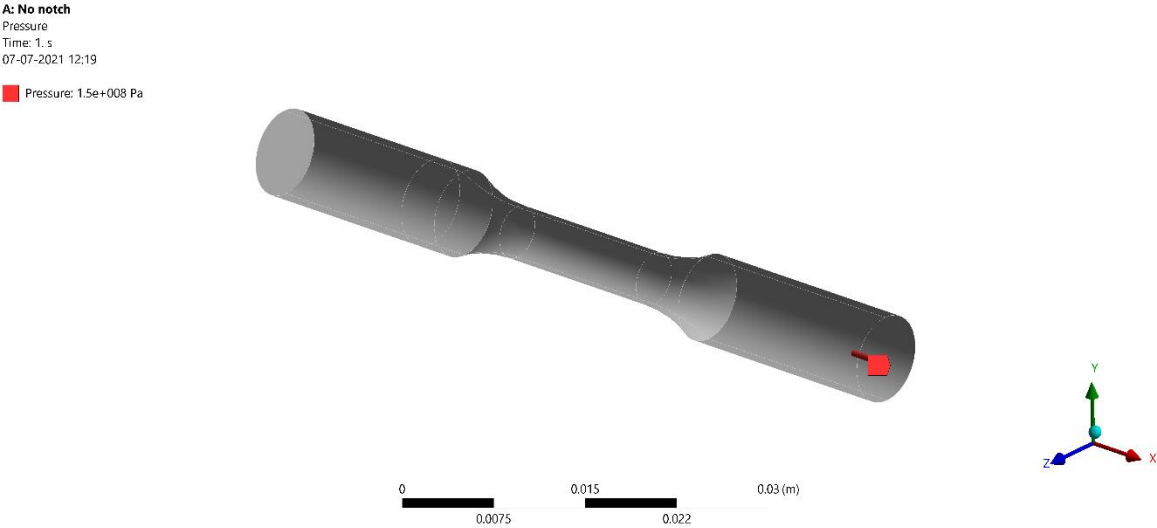


Fig 5.2 Loading on the standard specimen

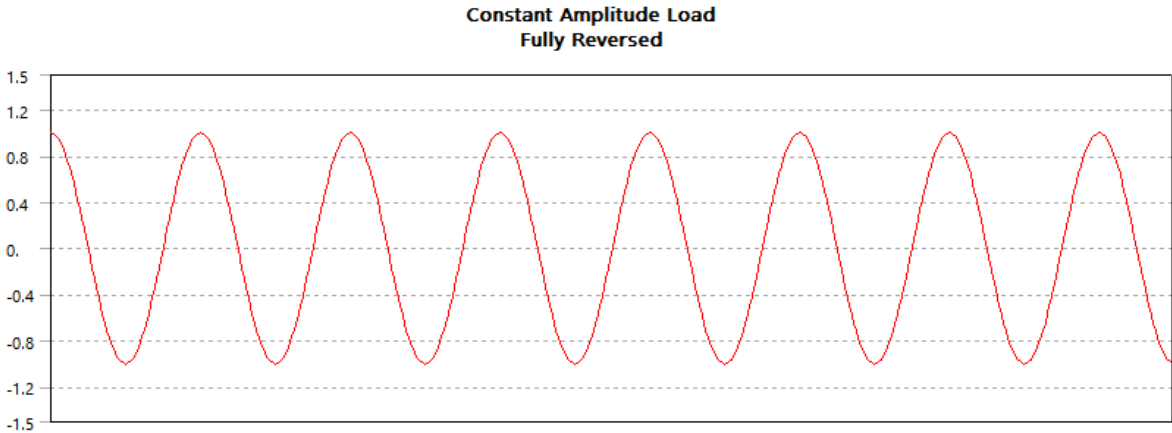


Fig 5.3 Constant Amplitude fully reversed loading

5.3 STRAIN BASED ANALYSIS IN ANSYS:

As the fatigue analysis is strain-based, the fatigue tool used for the estimation of fatigue life must be specified if the type of analysis is stress-based or strain-based. By default, the analysis type is set to stress-based and needs to be changed to strain-based fatigue analysis.

Details of "Fatigue Tool"	
Domain	
Domain Type	Time
Materials	
Fatigue Strength Factor (Kf)	1.
Loading	
Type	Fully Reversed
<input type="checkbox"/> Scale Factor	1.
Definition	
<input type="checkbox"/> Display Time	End Time
Options	
Analysis Type	Strain Life
Mean Stress Theory	None
Stress Component	Equivalent (von-Mises)
Infinite Life	1.e+009 cycles

Fig 5.4 Specification of strain life analysis in the Fatigue tool

5.3.1 MEAN STRESS EFFECT:

Strain life analysis must account to the effects of mean stresses of the cyclic load. There are two methods available in the fatigue tool of ANSYS solver in order to account for the mean stress effects produced in the material. They are namely:

1. Smith-Watson-Topper (SWT) approach
2. Morrow approach

However, in case of fully reversed type of cyclic loads, the magnitude of the maximum and minimum applied load in a cycle remains the same while the direction changes accordingly. Hence, the value of mean stress in case fully reversed loading is zero. Its magnitude being zero results in zero effects on the specimen due to the mean stress. Hence, using either of the two models or eliminating the consideration of mean stress effect in the analysis would result in the same approximation of fatigue life.

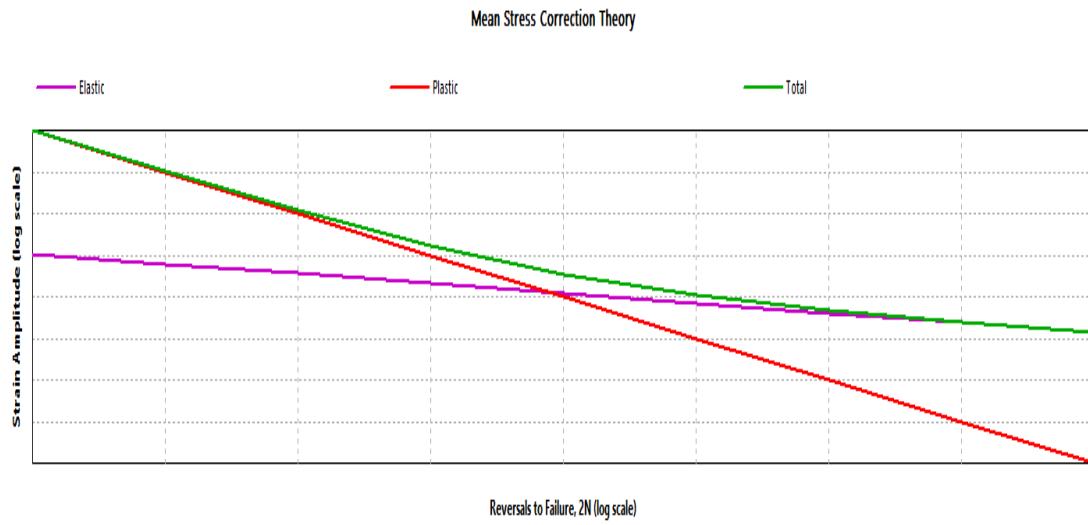


Fig 5.5 Mean stress correction

5.4 BOUNDARY CONDITIONS:

As mentioned in the section 5.2, one end of the specimen is fixed and the opposite end is acted upon by a fully reversed pressure load of 150 MPa.

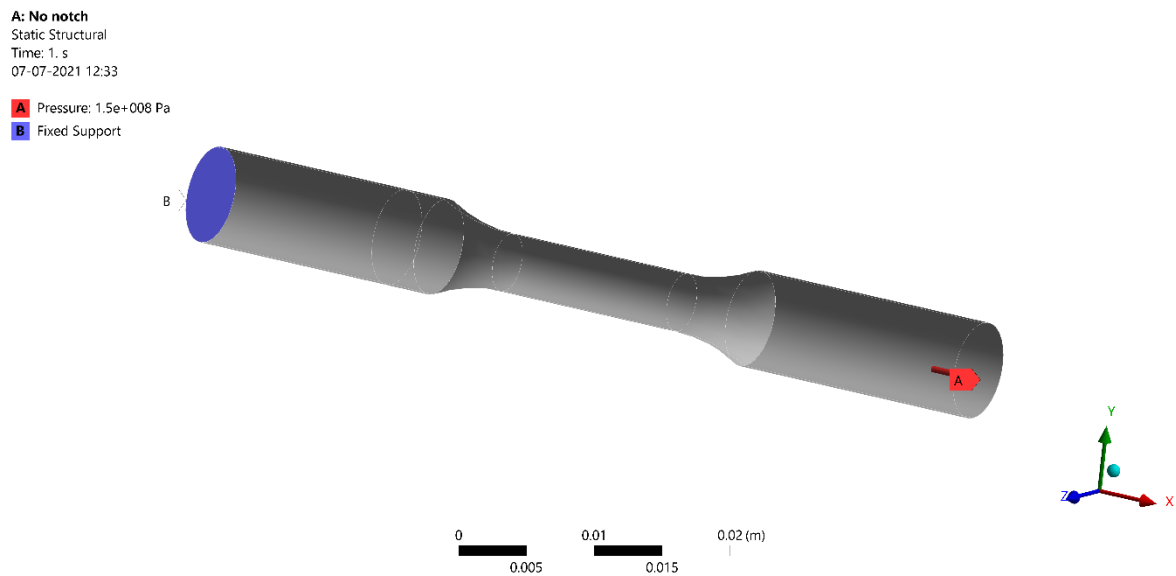


Fig 5.6 Boundary conditions on the fatigue specimen

5.5 MATERIAL ASSIGNMENT

5.5.1 UNS S32760:

Parameters used for the finite element fatigue analysis of UNS S32760 in ANSYS

Modulus of Elasticity (E): 200GPa

Poisson's Ratio (μ): 0.27

Fatigue strength coefficient (σ_f'): 1387.5 MPa

Fatigue strength exponent (b): -0.09

Fatigue Ductility coefficient (ϵ_f'): 0.32501

Fatigue ductility exponent (c): -0.56

Cyclic strain hardening exponent (n'): 0.16701

Cyclic strength coefficient (K'): 1662 MPa

5.6 NOTCH VARIATIONS:

Several types of V notches were made on the fatigue specimen by variation of notch parameters which are width(w), depth(d) and notch central angle(a). Geometry was prepared using the same 3D modelling software and were imported into ANSYS as IGES files. A total of 27 different notches were made by varying the width, depth and notch central angle. Same loading and boundary conditions were implemented in all the 27 cases and the fatigue life was estimated.

5.5.1 STRESS CONCENTRATION

Due to the notches that were put on the specimen, material develops high amounts of stress around the notched area and fails prematurely resulting in heavy losses. Hence, high variations can be observed in the fatigue life even if the notch is minute.

S.No	w	d	a	Pressure (MPa)	Equivalent Stress (Mpa)	Life
1	0.5	0.5	120	150	1057.8	1032
2	0.5	0.5	240	150	919.29	1990
3	0.5	0.5	360	150	1240.5	519
4	0.5	0.75	120	150	1257.6	490
5	0.5	0.75	240	150	1228	541
6	0.5	0.75	360	150	1604.5	187
7	0.5	1	120	150	1592	193
8	0.5	1	240	150	1550	214
9	0.5	1	360	150	1304.5	422
10	0.75	0.5	120	150	1088	910
11	0.75	0.5	240	150	995.36	1363
12	0.75	0.5	360	150	1289.6	442
13	0.75	0.75	120	150	1481.7	254
14	0.75	0.75	240	150	1267.5	474
15	0.75	0.75	360	150	1664.5	163
16	0.75	1	120	150	1409	310
17	0.75	1	240	150	1498.4	243
18	0.75	1	360	150	2578.4	34
19	1	0.5	120	150	1147.9	720
20	1	0.5	240	150	1388.3	328
21	1	0.5	360	150	2253.2	54
22	1	0.75	120	150	1051	1062
23	1	0.75	240	150	1364.8	351
24	1	0.75	360	150	1406	312
25	1	1	120	150	1197.9	600
26	1	1	240	150	1843.9	112
27	1	1	360	150	2264.2	54

Fig 5.7 Different variations of V notch and resulting fatigue life and equivalent stress

5.7 SOLUTION:

Two parameters were observed in the solution tab of ANSYS solver namely, the equivalent stress and fatigue life of the specimen. Initially, analysis was done without the notch in order to establish a ground reference of the fatigue life and equivalent stress under the applied load. The results obtained are as below:

A: No notch
 Equivalent Stress
 Type: Equivalent (von-Mises) Stress
 Unit: Pa
 Time: 1
 07-07-2021 12:56

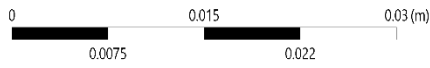
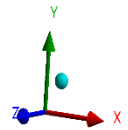
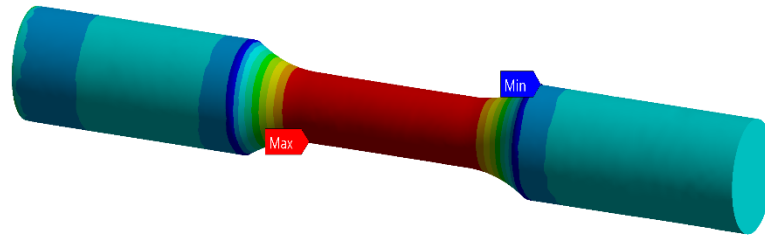
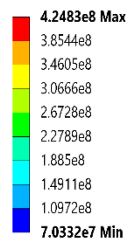


Fig 5.8 Equivalent stress developed in standard fatigue specimen

A: No notch
 Life
 Type: Life
 07-07-2021 12:56

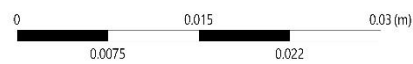
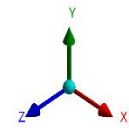
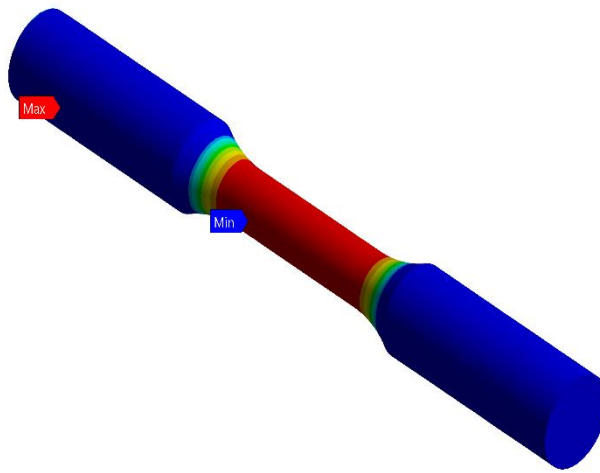
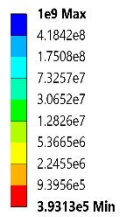


Fig 5.9 Strain based fatigue analysis of the standard fatigue test specimen

5.7.1 EXAMPLES OF ANALYSIS ON NOTCHED SPECIMEN

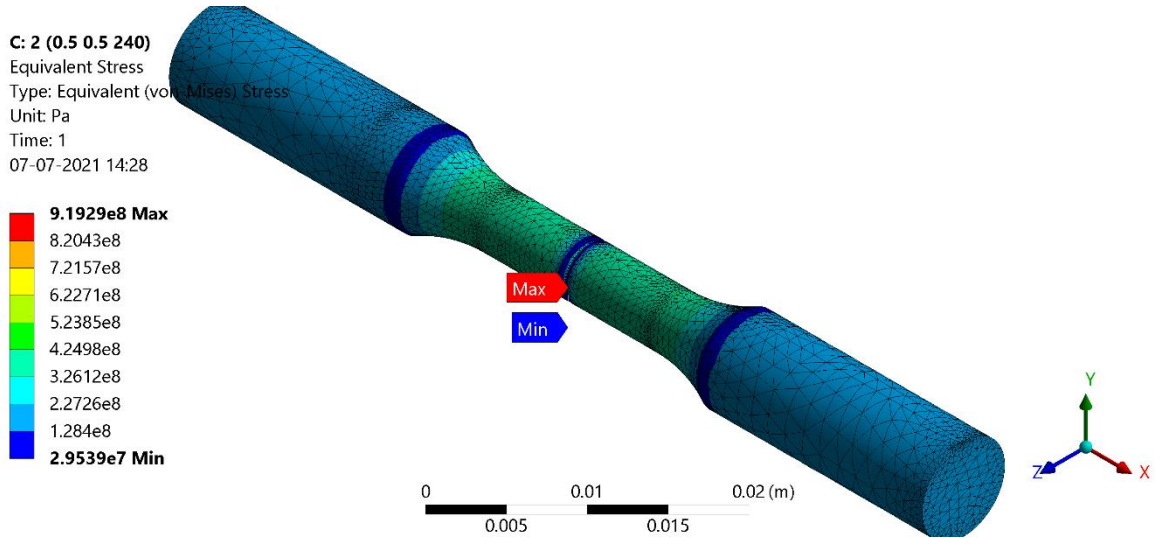


Fig 5.10 Equivalent stress generated in Notched specimen with $w=0.5\text{mm}$ $d=0.5\text{mm}$
 $a=240\text{ deg}$

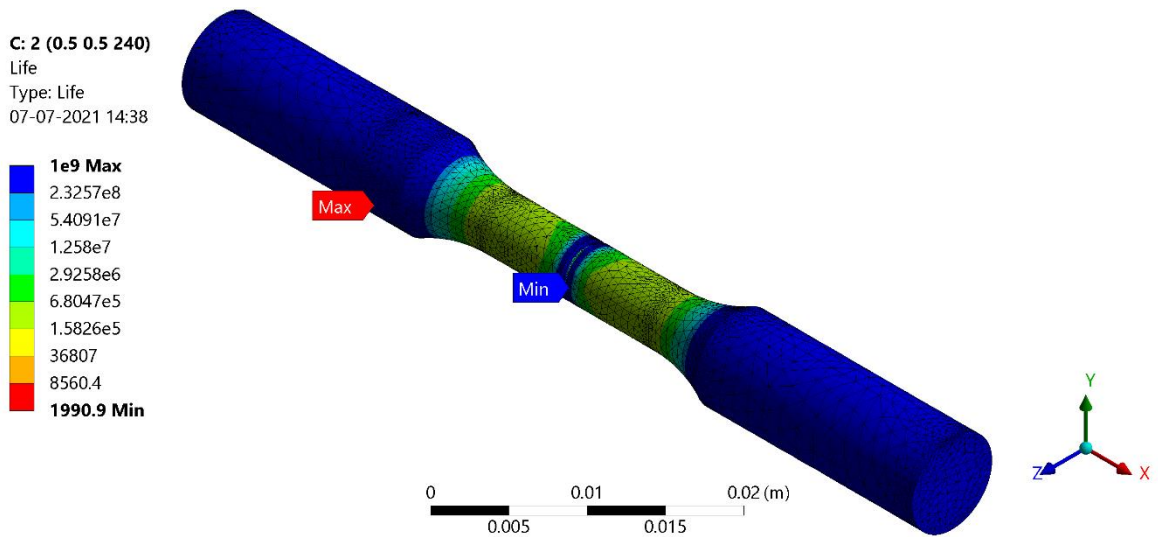


Fig 5.11 Fatigue life of Notched specimen with $w=0.5\text{mm}$ $d=0.5\text{mm}$ $a=240\text{deg}$

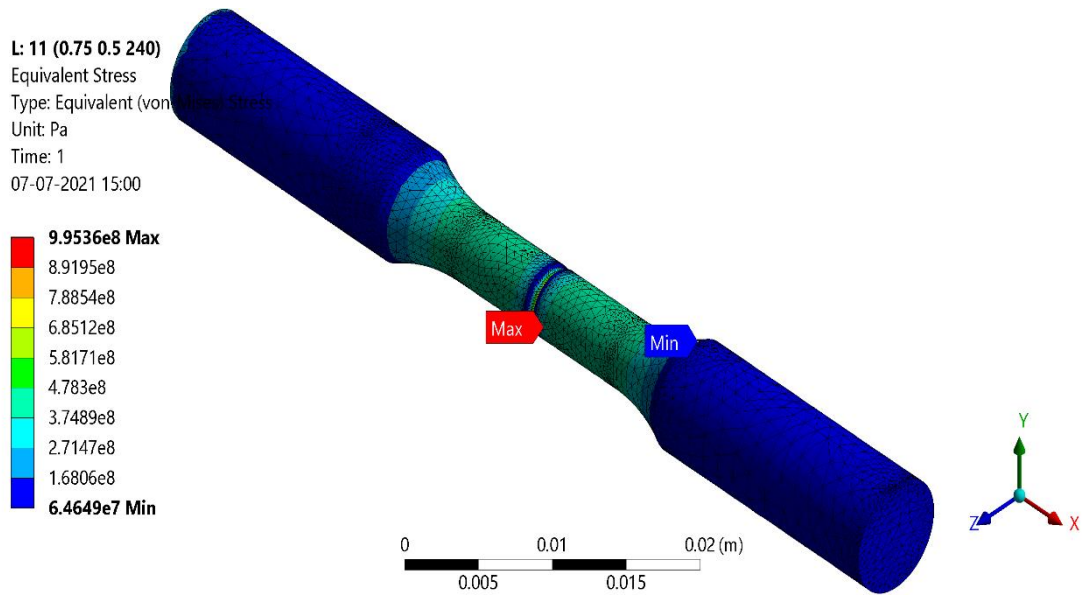


Fig 5.12 Equivalent stress generated in Notched specimen with $w=0.75\text{mm}$ $d=0.5\text{mm}$ $a=240\text{ deg}$

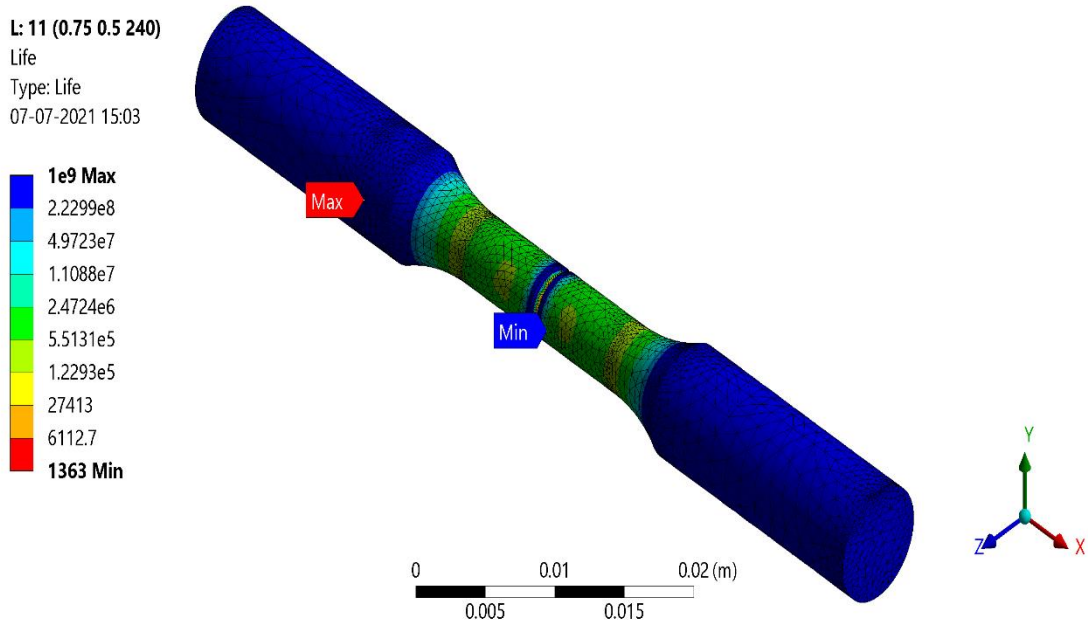


Fig 5.13 Fatigue life of Notched specimen with $w=0.75\text{mm}$ $d=0.5\text{mm}$ $a=240\text{ deg}$

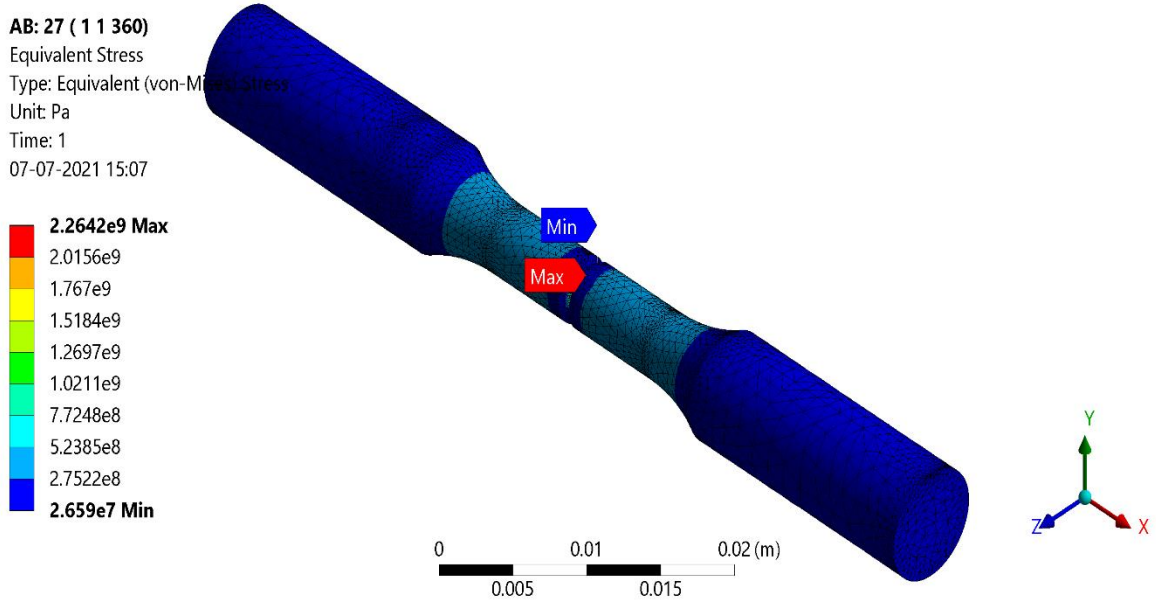


Fig 5.14 Equivalent stress generated in Notched specimen with $w=1\text{mm}$ $d=1\text{mm}$ $a=360\text{deg}$

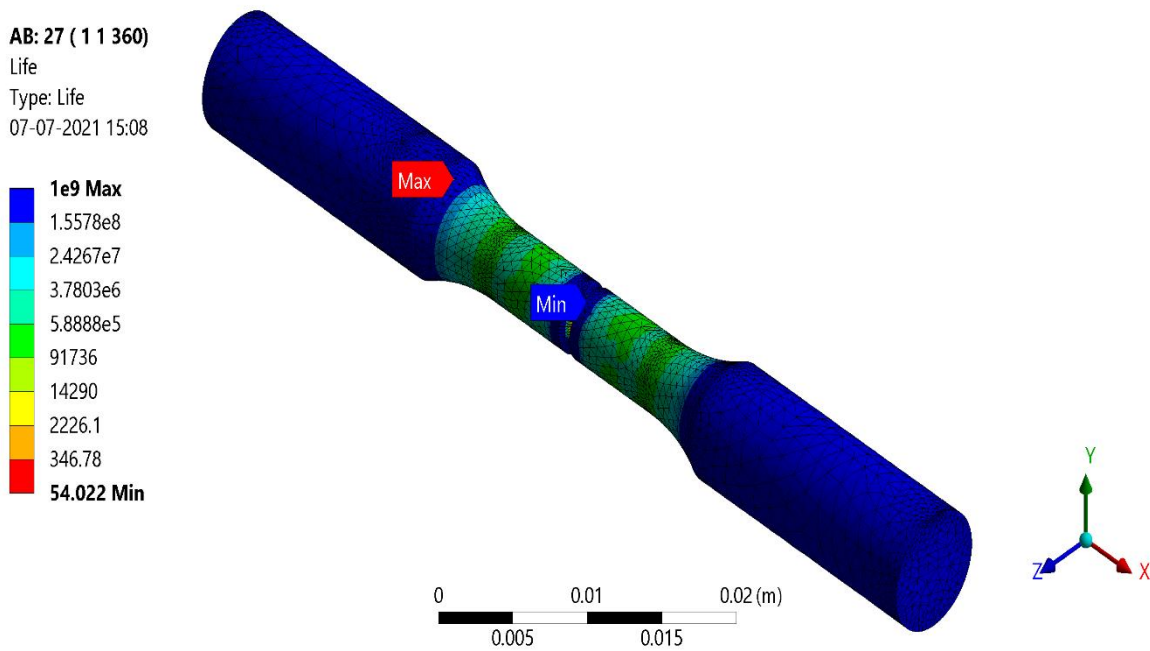


Fig 5.15 Fatigue life of Notched specimen with $w=1\text{mm}$ $d=1\text{mm}$ $a=360\text{ deg}$

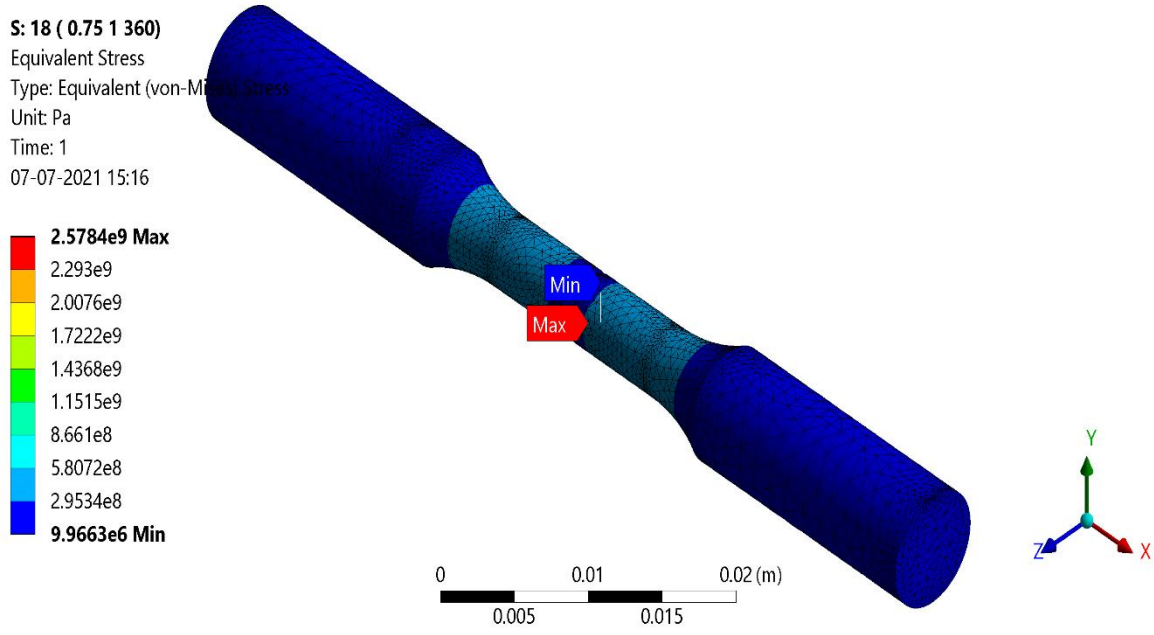


Fig 5.16 Equivalent stress generated in Notched specimen with $w=0.75\text{mm}$ $d=1\text{mm}$ $a=360\text{deg}$

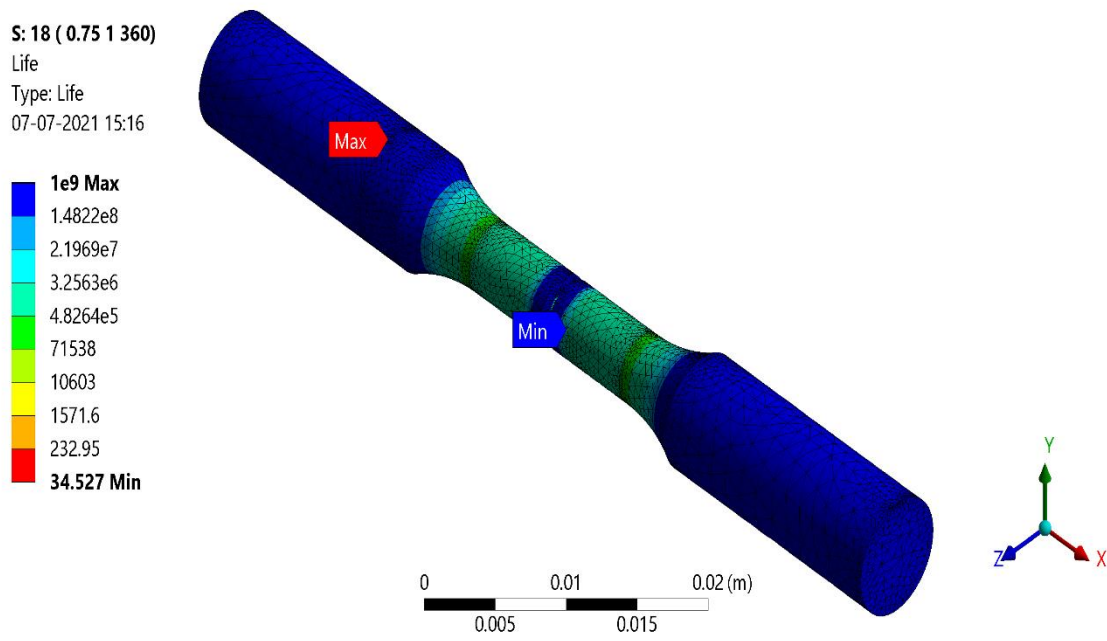


Fig 5.17 Fatigue life of Notched specimen with $w=0.75\text{mm}$ $d=1\text{mm}$ $a=360\text{deg}$

CHAPTER 6: RESULTS

6.1 TAGUCHI OPTIMIZATION:

Using the MINITAB application, Taguchi analysis was performed on the 27 notch variations mentioned in Table 3.2. The factor is the fatigue life while the predictors being notch parameters (width, depth and notch central angle). Following results were obtained after the analysis:

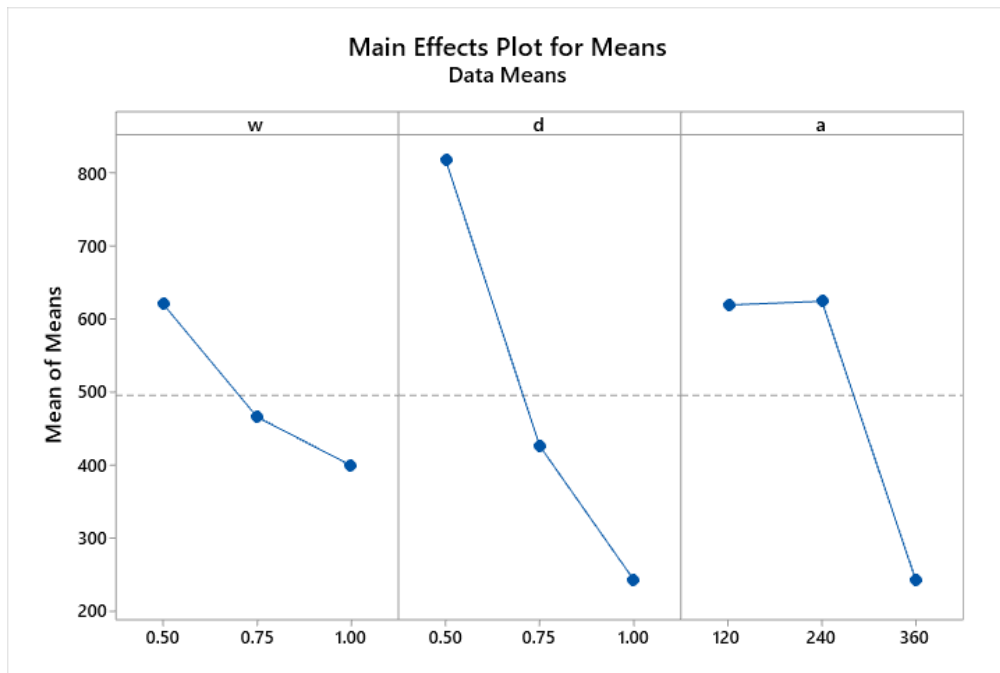


Fig 6.1 Variation of fatigue life with width, depth and Notch central angle

6.1.1 Response Table for Means

Level	w	d	a
1	620.9	817.6	650.3
2	465.9	426.0	522.1
3	399.2	242.4	313.6
Delta	221.7	575.1	336.8
Rank	3	1	2

Table 6.1 Response table indicating the influence level of each notch parameter

6.2 REGRESSION ANALYSIS:

6.2.1 REGRESSION EQUATION:

$$f = 3252 - 356 w - 3141 d - 7.22 a + 324 w*d + 0.47 w*a + 7.40 d*a$$

Where, W = Width

D = Depth and

A = Notch central angle

6.2.2 ANALYSIS OF VARIANCE:

Source	DF	Adj SS	Adj MS	F-Value	P-Value
Regression	6	2604038	434006	3.34	0.019
w	1	4527	4527	0.03	0.854
d	1	353172	353172	2.72	0.115
a	1	76379	76379	0.59	0.452
w*d	1	1434	1434	0.01	0.917
w*a	1	705	705	0.01	0.942
d*a	1	172568	172568	1.33	0.263
Error	20	2600786	130039		
Lack-of-Fit	2	103343	51671	0.37	0.694
Pure Error	18	2497443	138747		
Total	26	5204824			

Table 6.2 ANOVA table for the considered data set

6.3 RESPONSE SURFACE METHODOLOGY:

6.3.1 REGRESSION EQUATION IN UNCODED UNITS:

$$f = 6862 - 7628 w - 7743 d + 3.0 a + 2206 w*w + 786 d*d - 0.0069 a*a + 6240 w*d - 3.73 w*a + 1.60 d*a$$

where, w = width

d = depth and

a = Notch central angle.

6.3.2 ANALYSIS OF VARIANCE:

Source	DF	Adj SS	Adj MS	F-Value	P-Value
Model	9	2461465	273496	1.54	0.331
Linear	3	1670962	556987	3.13	0.126
w	1	142311	142311	0.80	0.412
d	1	1125000	1125000	6.32	0.054
a	1	403651	403651	2.27	0.192
Square	3	122935	40978	0.23	0.872
w*w	1	70189	70189	0.39	0.558
d*d	1	8911	8911	0.05	0.832
a*a	1	36280	36280	0.20	0.671
2-Way Interaction	3	667568	222523	1.25	0.385
w*d	1	608400	608400	3.42	0.124
w*a	1	49952	49952	0.28	0.619
d*a	1	9216	9216	0.05	0.829
Error	5	890032	178006		
Lack-of-Fit	3	890032	296677	*	*
Pure Error	2	0	0		
Total	14	3351498			

Table 6.3 ANOVA of RSM

6.3.3 SURFACE PLOTS OF RSM:

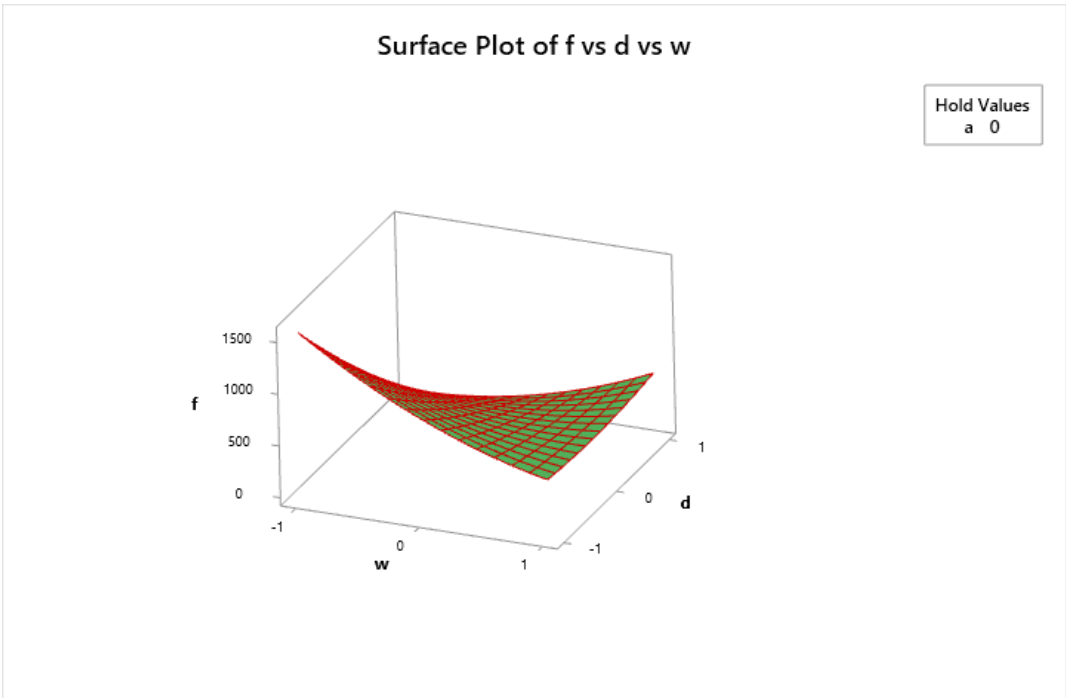


Fig 6.2 Surface plot of fatigue life vs width vs depth

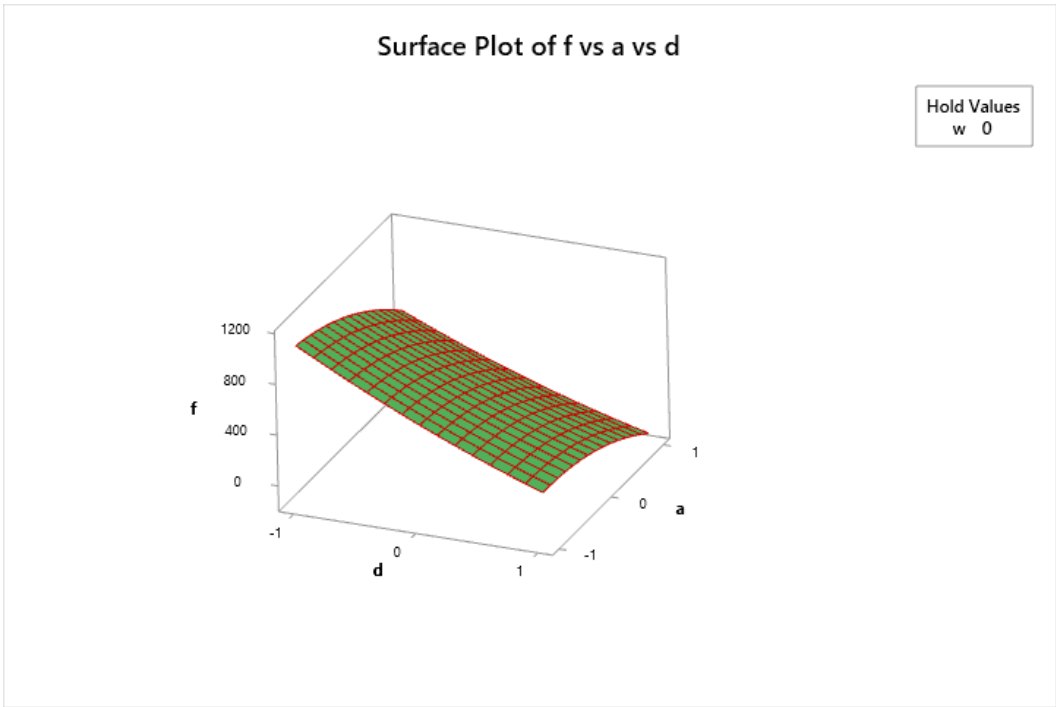


Fig 6.3 Surface plot of fatigue life vs Notch central angle vs depth

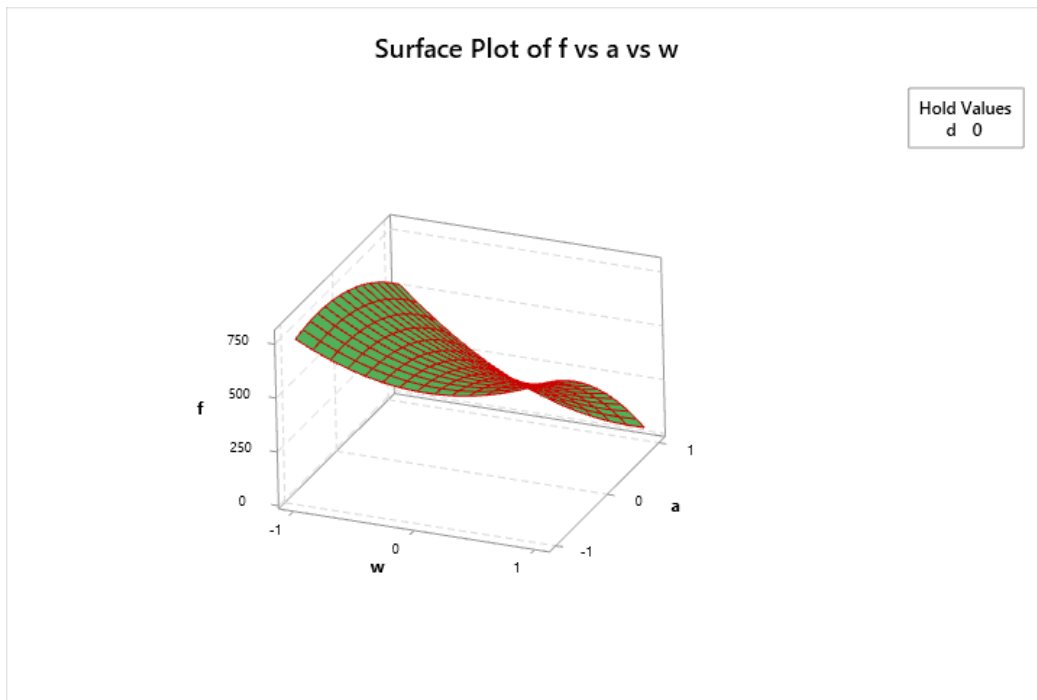


Fig 6.4 Surface plot of fatigue life vs width vs notch central angle

6.3.4 CONTOUR PLOTS:

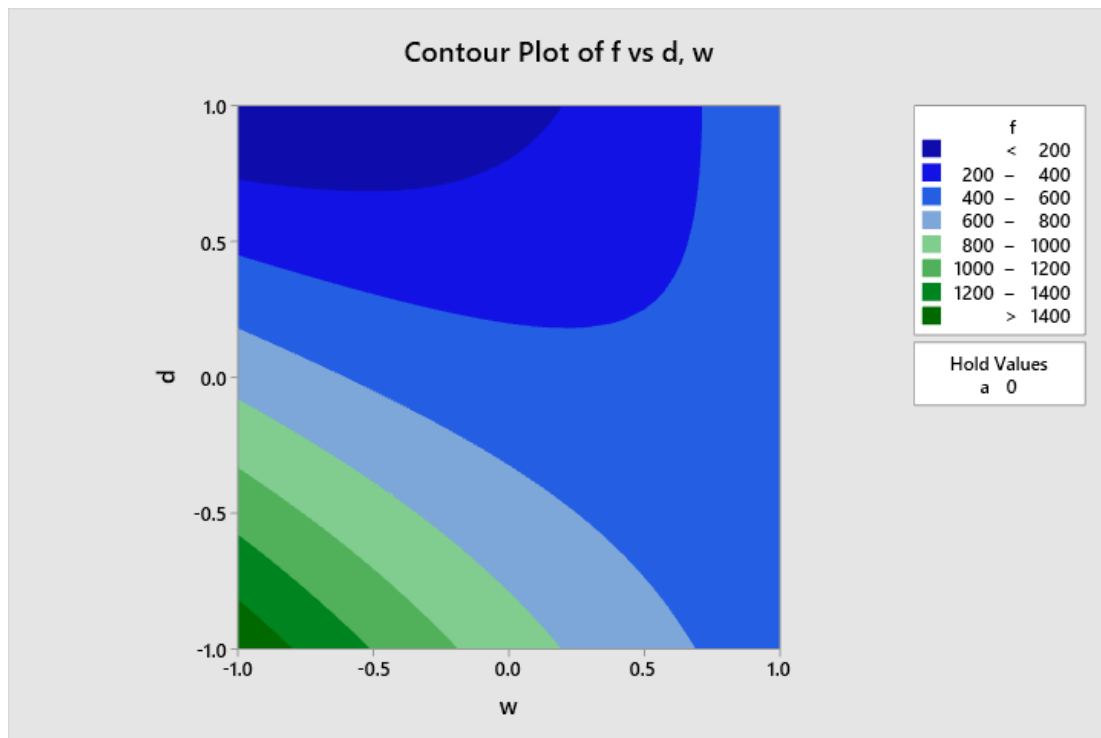


Fig 6.5 Contour plot of Fatigue life vs depth and width

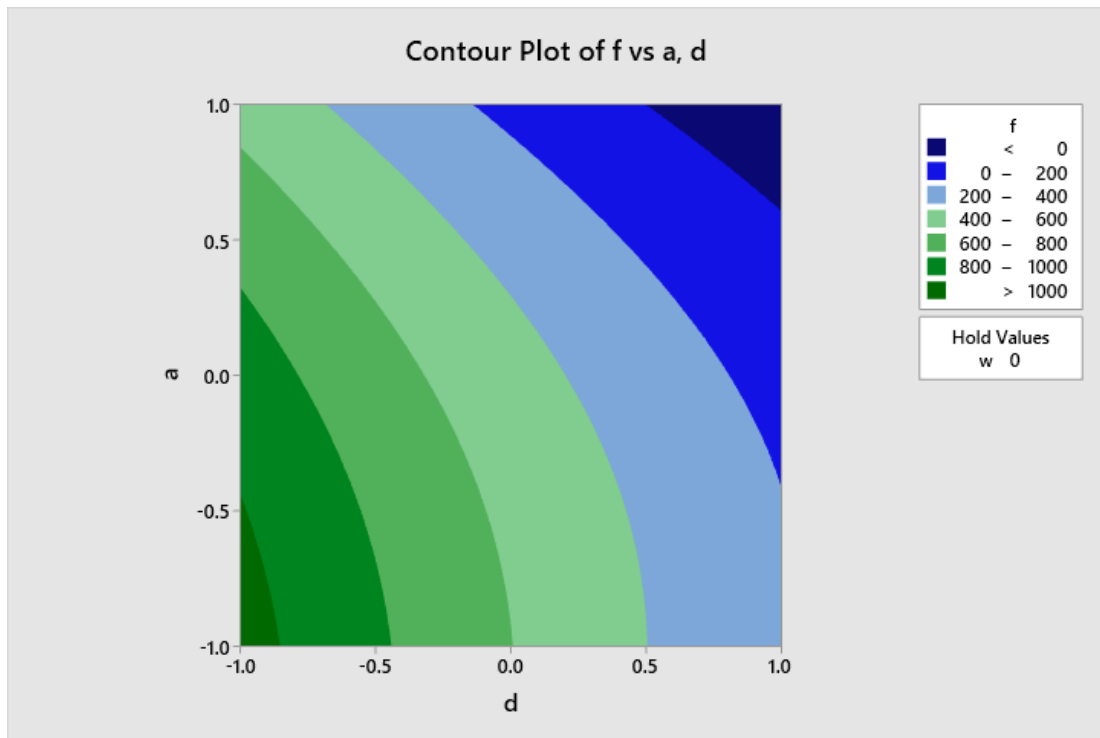


Fig 6.6 Contour plot of Fatigue life vs Notch central angle and Depth

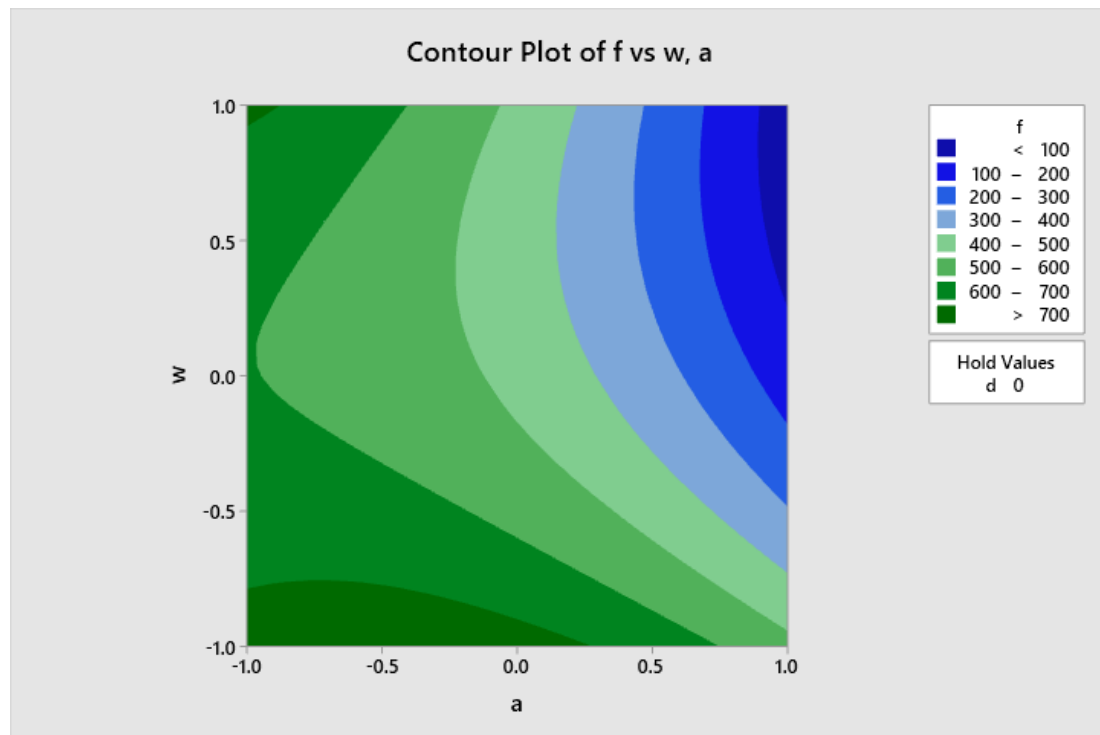


Fig 6.7 Contour plot of fatigue life vs width and notch central angle

CHAPTER 7: CONCLUSION

- From the graph in Fig.6.1, Fatigue life is maximum when width of the notch is minimum, depth of the notch is minimum and notch central angle is close to 240 degrees.
- The response table indicates that the depth of the V- notch affects fatigue life the most followed by the notch central angle and width of the notch.
- The surface plots obtained from response surface methodology indicate the following
 - ❖ Fatigue life is maximum when the depth and width of the notch is minimum and fatigue life is minimum when width is minimum and depth is maximum.
 - ❖ Fatigue life is also maximum when depth of the notch is minimum and notch central angle is close to the average value
 -
 - ❖ Fatigue life is also maximum when width of the notch is minimum and notch central angle is close to the average value.
- As mentioned in Chapter 4, the numerical method used in this analysis to calculate the fatigue constants (Universal Slopes method) is only for initial analysis and not to be used for design purposes. Due to this, the calculated fatigue life values may deviate considerably from their actual values. To eliminate this deviation all the fatigue properties must be obtained experimentally.
- The fatigue life equations obtained by regression analysis and RSM may be used to estimate the fatigue life of notched components with considerable accuracy.

REFERENCES

1. M. Kamal and M M Rahman (2018), “Advances in fatigue life modelling: A review”, *Renewable and sustainable energy reviews*, 82: pp 940-949.
2. Ernianzhao, Qiangzhou, Weilian Qu, and Wenming Wang (2020), “Fatigue properties estimation, life prediction for steels under axial, torsional and phase loading”, *Hindawi advances in material science and engineering*, Article ID 8186159.
3. J.H Ong, “An evaluation of existing methods for the prediction of axial fatigue life from tensile data”, *Int J Fatigue* 15 No 1 (1993) pp 13-19
4. Jun-Hyub Park and Ji-Ho Song, “Detailed evaluation of methods for estimation of fatigue properties”, *Int. J. Fatigue* Vol, 17, No. 5, pp. 365-373, 1995
5. N. Shamsei and A. Fatemi, (2009), “Effect of hardness on multiaxial fatigue behaviour and some simple approximations for steels”, *Fatigue and Fracture of Engineering Materials and Structures* 32, pp 631–646
6. Kamaya, M., Kawakubo, M., Mean stress effect on fatigue strength of stainless steel, *International Journal of Fatigue* (2014)
7. C.R Williams, Y.L Lee, J.T Rilly, “A practical method for statistical analysis of strain life fatigue data”, *International Journal of Fatigue* 25 (2003) pp 427–436
8. Zhongping Zhang, Yanjiang Qiao, Qiang Sun, Chunwang Li and Jing Li, (2009), “Theoretical Estimation to the cyclic strength coefficient and the Cyclic Strain hardening Exponent for Metallic Materials: Preliminary Study”, *Journal of Materials Engineering and Performance*, Volume 18(3), pp 245-254
9. M.L Roessle, A. Fatemi, “Strain-controlled fatigue properties of steels and some simple approximations”, *International Journal of Fatigue* 22 (2000) 495–511

10. M.A Meggiolaro, J.T.P. Castro, “Statistical evaluation of strain-life fatigue crack initiation predictions”, *International Journal of Fatigue* 26 (2004) 463 -476
11. S.S. Manson, “Fatigue: A complex subject- Some Simple Approximations”, *The William M. Murray Lecture, 1964*
12. K.S. Kim, X. Chen, C. Han, H.W. Lee, “Estimation methods for fatigue properties of steels under axial and torsional loading”, *International Journal of Fatigue* 24 (2002) 783–793
13. Yung-Li Lee, Mark E. Barkey, (2012). *Strain based uniaxial Fatigue Analysis, Chapter-6*, Elsevier.
14. Howard E. Boyer, Atlas of Fatigue Curves, *American Society for Metals International*, pp. 9, 2006.
15. Bruce Boardman, Properties and Selection: Irons, Steels, and High-Performance Alloys, *ASM Handbook, Vo. 1*, pp. 673-688, 1990.
16. Ian F.C. Smith, Manfred A. Hirt, A review of fatigue strength improvement methods, *Canadian Journal of Civil Engineering, Vol. 12, Issue 1*, pp. 166-183, 2011.
17. Mitchell P. Kaplan, Timothy A. Wolff, Fatigue-Life Assessment, Failure Analysis and Prevention, *Vol. 11, ASM Handbook, ASM International*, pp. 276-288, 2002.
18. F.C. Campbell, Elements of Metallurgy and Engineering Alloys, *ASM International, Vol. 83, Issue 1*, pp. 317, 2008.
19. X.W. Ye, Y.H. Su, J.P. Han, A State-of-the-Art Review on Fatigue Life Assessment of Steel Bridges, *Mathematical Problems in Engineering, Volume 2014, Article ID 956473*, 2014.
20. T.L. Anderson, Fracture Mechanics Fundamentals and Applications, *3rd Edition, Taylor & Francis*, 2005.

21. Walter G. Reuter, Robert S. Piascik, Fatigue & Fracture Mechanics: 33rd Volume, *ASTM International*, 2002.
22. C.S. Yen, T.J. Dolan A Critical Review of the Criteria for Notch-Sensitivity in Fatigue of Metals, University of Illinois Engineering Experiment Station, *Bulletin Series No. 898*, Vol. 49, Issue 53, 1952.
23. R. Sunder, Spectrum load fatigue – underlying mechanisms and their significance in testing and analysis, *International Journal of Fatigue*, Vol. 25, pp. 971–981, 2003.
24. A. Fatemi, L. Vang, Cumulative fatigue damage and life prediction theories: a survey of the state of the art for homogeneous materials, *International Journal of Fatigue*, Vol. 20, Issue 1, 1998.
25. Ralph I. Stephens, Ali Fatemi, Robert R. Stephens, Henry O. Fuchs, Metal Fatigue in Engineering, 2nd Edition, ISBN: 978-0-471-51059-8, 2000.
26. Richard P. Wool, Fundamentals of Fracture in Bio-Based Polymers, Bio-Based Polymers and Composites 1st Edition, *Academic Press*, pp. 149-201, 2005.
27. Xian-Kui Zhu, James A. Joyce, Review of fracture toughness (G, K, J, CTOD, CTOA) testing and standardization, *Engineering Fracture Mechanics*, Vol. 85, pp. 1-46, 2012
28. W. Elber, The Significance of Fatigue Crack Closure, Damage Tolerance in Aircraft Structures, *West Conshohocken, ASTM International*, pp. 230-242, 1971
29. Bong-Ryul You, Soon-Bok Lee, A critical review on multiaxial fatigue assessments of metals, *International Journal of Fatigue*, Vol. 18, Issue 4, pp. 235-244, 1996.
30. M.T. Yu, D.L. DuQuesnay, T. H. Topper, Notch fatigue behaviour of SAE1045 steel, *Int. J. Fatigue*, vol. 10, no. 2, pp. 109–116, 1988.
31. M.Makkonen, Notch size effects in the fatigue limit of steel, *International Journal of Fatigue*, Vol. 25, Issue 1, pp. 17–26, 2002.

32. Y.T. Li, B. Chen, and C.F. Yan, Effect of Parameters of Notch on Fatigue Life of Shaft Based on Product Lifecycle Management, *Materials Science Forum*, Vol. 638, pp. 3864–3869, 2010.
33. N. Mamidi, J.J. Kumar, R.Nethi, and V.Kadali, Impact of Notch Depth on the Fatigue Life of AISI 316L Austenitic Stainless Steel, *International Research Journal of Engineering and Technology*, Vol. 5 Issue 9, pp. 1149-1151, 2018.
34. D.Radaj, Review of fatigue strength assessment of nonwelded and welded structures based on local parameters, *International Journal of Fatigue*, Vol. 18, Issue 3, pp. 153–170, 1996.
35. K.Schoenborn, Fatigue Analysis of a Welded Assembly Using ANSYS Workbench Environment, *October 2006*.
36. P.Heyes and J.Mentley, Fatigue Analysis of Seam Welded Structures using nCodeDesignLife, *nCode*, pp. 1–21, 2013.
37. Ronald H. Schmidt, Daniel J. Erickson, Steven Sims, Philip Wolf, Characteristics of Food Contact Surface Materials: Stainless Steel, *Food Protection Trends*, Vol. 32, Issue 10, pp. 574–584, 2012.
38. Design Guidelines for the Selection and use of Stainless Steel, *A Designers' Handbook Series No: 9014, Nickel Development Institute, 1991*.
39. Flake C. Campbell, Elements of Metallurgy and Engineering Alloys, *ASM International, 2008*.
40. Standard Test Method for Strain-Controlled Fatigue Testing, *E606/E606M-12 standard, ASTM International*.
41. Taguchi Techniques for Quality Engineering, 2nd Edition, Phillip J. Ross, *McGraw Hill Professional, 1996*.